



Final Report SPR-FY23(016)

Nebraska Balanced Mix Design - Phase II

Farzad Yazdipناه, M.S.

Graduate Research Assistant
Department of Civil & Environmental
Engineering
University of Nebraska-Lincoln

Jamilla Emi Sudo Lutf Teixeira, Ph.D.

Assistant Professor
Department of Civil & Environmental
Engineering
University of Nebraska-Lincoln

Mahdieh Khedmati, Ph.D.

Research Engineer
Department of Civil & Environmental
Engineering
University of Nebraska-Lincoln

Hamzeh F. Haghshenas, Ph.D.

Adjunct Professor
Department of Civil & Environmental
Engineering
University of Nebraska-Lincoln

Nebraska Department of Transportation Research

Headquarters Address (402) 479-4697
1400 Nebraska Parkway [https://dot.nebraska.gov/
Lincoln, NE 68509 business-center/research/](https://dot.nebraska.gov/business-center/research/)
ndot.research@nebraska.gov

Nebraska Transportation Center

262 Prem S. Paul Research (402) 472-1932
Center at Whittier School <http://ntc.unl.edu>
2200 Vine Street
Lincoln, NE 68583-0851

This report was funded in part through grant from the U.S. Department of Transportation Federal Highway Administration. The views and opinions of the authors expressed herein do not necessarily state or reflect those of the U.S. Department of Transportation.

Nebraska Balanced Mix Design – Phase II

Farzad Yazdipanah, M.S.
Graduate Research Assistant
Department of Civil & Environmental Engineering
University of Nebraska-Lincoln

Mahdieh Khedmati, Ph.D.
Research Engineer
Department of Civil & Environmental Engineering
University of Nebraska-Lincoln

Jamilla Emi Sudo Lutf Teixeira, Ph.D.
Assistant Professor
Department of Civil & Environmental Engineering
University of Nebraska-Lincoln

Hamzeh F. Haghshenas, Ph.D.
Adjunct Professor
Department of Civil & Environmental Engineering
University of Nebraska-Lincoln

Sponsored By

Nebraska Department of Transportation and US Department of Transportation Federal Highway
Administration

May 2025

Technical Report Documentation Page

1. Report No. SPR-FY23(016)	2. Government Accession No.	3. Recipient's Catalog No.	
4. Title and Subtitle Nebraska Balanced Mix Design – Phase II		5. Report Date May 31, 2025	
		6. Performing Organization Code	
7. Author(s) Farzad Yazdipanah, Mahdieh Khedmati, Jamilla Teixeira, and Hamzeh F. Haghshenas		8. Performing Organization Report No. 26-1121-4060-001	
9. Performing Organization Name and Address University of Nebraska-Lincoln Department of Civil Engineering Scott Engineering Center, 844 N 16th St., C190, Lincoln, NE 68588-0531		10. Work Unit No.	
		11. Contract	
12. Sponsoring Agency Name and Address Nebraska Department of Transportation 400 Highway 2, PO Box 94759, Lincoln, NE 68509		13. Type of Report and Period Covered Final Report 07/2022 - 05/2025	
		14. Sponsoring Agency Code	
15. Supplementary Notes			
16. Abstract <p>This study aimed to propose a performance-based framework to evaluate highly recycled asphalt mixtures containing polymer-modified binders for potential use in a balanced mix design (BMD) specification in the state of Nebraska. For that, loose and compacted mixtures were directly collected from plant and field projects within a benchmarking study, subjected to an extensive experimental program. The laboratory investigation employed different monotonic tests recommended in BMD Phase 1, as well as the dynamic modulus test. Three long-term aging protocols were investigated in terms of their impact on the mechanical, rheological, and chemical characteristics of asphalt mixtures and binders. Moreover, field assessments with cores and pavement management system data were added to the analysis. Results evaluated the sensitivity and significance of various tests for characterizing rutting and cracking resistance across mixtures varying in binder sources, grades, recycled contents, and warm mix additives. The variability and discrimination potential of performance-based parameters were identified, and suitable performance tests were suggested for the BMD framework considering the type of mixtures and site conditions of this study. The preliminary threshold criteria for each performance test were selected using a mechanistic-empirical approach considering three representative structural layers. Regarding the aging protocol, while the studied aging protocols yielded similar cracking resistance trends, their aging severity differed. Considering mechanical, chemical, and rheological similarities, an adjusted long-term aging protocol was selected for the potential implementation in the state's BMD framework. Reheating and dwelling time impacted performance indices, showing they could be considered in criteria selection. The selected performance-based parameters and threshold criteria corroborated with the results from field rutting, roughness, and cracking assessments, which further verify the outcomes. It was recommended to validate the selected performance tests, associated preliminary criteria, and aging protocol using more extended field data collection.</p>			
17. Key Words Balanced Mix Design, Rutting, Fatigue Cracking, Long-term Aging, Mechanistic empirical pavement design, Preliminary criteria		18. Distribution Statement No restrictions. This document is available through the National Technical Information Service. 5285 Port Royal Road Springfield, VA 22161	
19. Security Classification (of this report) Unclassified	20. Security Classification (of this page) Unclassified	21. No. of Pages 101	22. Price

Disclaimer

The contents of this report reflect the views of the authors, who are responsible for the facts and the accuracy of the information presented herein. The contents do not necessarily reflect the official views or policies neither of the Nebraska Department of Transportations nor the University of Nebraska-Lincoln. This report does not constitute a standard, specification, or regulation. Trade or manufacturers' names, which may appear in this report, are cited only because they are considered essential to the objectives of the report.

The United States (U.S.) government and the State of Nebraska do not endorse products or manufacturers. This material is based upon work supported by the Federal Highway Administration under SPR-FY23 (016). Any opinions, findings and conclusions or recommendations expressed in this publication are those of the author(s) and do not necessarily reflect the views of the Federal Highway Administration.

This report has been reviewed by the Nebraska Transportation Center for grammar and context, formatting, and 508 compliances.

Table of Contents

Technical Report Documentation Page	i
Disclaimer	ii
Table of Contents	iii
List of Figures	v
List of Tables	vii
Acknowledgments.....	viii
Abstract	ix
Chapter 1 Introduction	1
1.1 Research Objectives.....	7
1.1.1 Step 1: Laboratory Assessment of NE Mixtures Using Different Performance Tests.....	7
1.1.2 Step 2: Validation of Performance Test Results Based on Field Assessment	8
1.1.3 Step 3: Selecting Preliminary Threshold Criteria and Appropriate LTA Protocol	8
1.2 Organization of the Report.....	10
Chapter 2 Summary of Nebraska BMD Phase 1 Project	11
Chapter 3 Site Location, Materials, and Test Methods.....	13
3.1 Materials, Projects, and Site Locations.....	13
3.2 Performance Test Methods and Aging Protocols	16
3.2.1 Dynamic Modulus (DM) Test.....	16
3.2.2 Hamburg Wheel Tracking Test (HWTT)	17
3.2.3 Indirect Tensile Asphalt Rutting Test (IDEAL-RT).....	18
3.2.4 Illinois Flexibility Index Test (IFIT).....	19
3.2.5 Indirect Tensile Asphalt Cracking Test (IDEAL-CT)	20
3.2.6 Short-term Aging (STA) and Long-term Aging (LTA) Protocols.....	21
3.3 I-FIT (AASHTO - T 393)	23
Chapter 4 Laboratory Test Results and Discussion	24
4.1 Step 1: Laboratory Assessment of NE Mixtures using Different Performance Tests	24
4.1.1 Dynamic Modulus Test Results	24
4.1.2 Rutting Test Results	27
4.1.3 Cracking Test Results	31
4.2 Step 2: Validation of Performance Tests Results Based on Field Assessment.....	38
4.3 Summary of the Tests' Key Characteristics.....	43
Chapter 5 Preliminary Threshold Criteria for Performance Tests	45
5.1 Introduction to the MEPDG Method	45
5.1.1 Distress Prediction Equations for Flexible and Semi-Rigid Pavements	48
5.1.2 Rutting Depth.....	48
5.1.3 Load-Related Cracking	49
5.1.4 Non-Load-Related Cracking-Transverse Cracking	51
5.1.5 Reflective Cracking in HMA Overlays.....	52
5.2 Design Inputs and Structural Layer Properties Considered in this Project.....	54
5.3 Validation of MEPDG Assumptions using Field Data	58
5.4 Defining Performance Tests' Threshold using MEPDG Approach	63
5.4.1 PCC-Structure-1 st Scenario	65
5.4.2 PCC-Structure-2 nd Scenario (with a thin fine-graded mixture layer)	67

5.4.3 Non-PCC Structure	70
Chapter 6 Long-Term Aging Protocol Selection.....	73
6.1 Mechanical Test Assessment of LTA Protocol	73
6.2 Rheological and Chemical Test Assessment of LTA Protocol.....	75
Chapter 7 Research Conclusion and Future Works	81
References	83

List of Figures

Figure 1.1 Experimental plan adopted in this study.	9
Figure 3.1 Aggregate gradation and criteria (a) mix A, B, E and (b) mix C, D, F	15
Figure 3.2 Site location of the selected projects in this study.....	15
Figure 3.3 DM test setup and sample preparation	17
Figure 3.4 HWTT setup and sample preparation.....	17
Figure 3.5 IDEAL-RT test setup and sample conditioning	18
Figure 3.6 IFIT setup and sample preparation procedure	20
Figure 3.7 IDEAL-CT setup and sample sample geometry before and after running the test	21
Figure 4.1 Master curves at 21 °C: (a) $ E^* $ and (b) δ	24
Figure 4.2 (a) $ E^* $ value at 38 °C and 0.1 Hz, (b) G-R _m parameter at 20 °C and 5 Hz.....	26
Figure 4.3 Rutting test results: (a) Rut depth (HWTT), and (b) <i>RTIndex</i> (IDEAL-RT).....	27
Figure 4.4 Correlation between DM vs. HWTT and DM vs. IDEAL-RT	29
Figure 4.5 FI results for lab compacted specimens (STA and LTA).....	32
Figure 4.6 <i>CTIndex</i> results for lab compacted specimens (STA and LTA)	33
Figure 4.7 Correlation between (a) G-R _m vs. <i>CTIndex</i> , G-R _m vs. FI, and (b) FI vs. <i>CTIndex</i> ...	37
Figure 4.8 IDEAL-RT and HWTT results of field core specimens during service life.....	39
Figure 4.9 The PMS data during service life (a) IRI, and (b) rut depth.....	41
Figure 4.10 IDEAL-CT and I-FIT results of field core specimens during service life	43
Figure 5.1 Conceptual Flowchart of the Three-Stage Design/Analysis Process for AASHTOWare (Adopted from [64]).....	46
Figure 5.2 Traffic data (AADTT) adoption for each project.....	55
Figure 5.3 Projects' structural layers for mechanistic-empirical pavement design	56
Figure 5.4 a) soil types in Nebraska and project locations, and b) resilient modulus vs. Nebraska group index of soils [67]	57
Figure 5.5 Road section and lane numbers (pictures adopted from Google map): a) LA, N-121, Crofton North, b) LD, US-75, Tekamah, c) LE, Highway 2, Grand Island to Cairo, d) LF, US-74, Ong spur.....	57
Figure 5.6 Mechanistic-empirical pavement design and PMS data for LA project (Crofton)	59
Figure 5.7 Mechanistic-empirical pavement design and PMS data for LD project (Tekamah) ...	60
Figure 5.8 Mechanistic-empirical pavement design and PMS data for LE project (Grand Island)	61
Figure 5.9 Mechanistic-empirical pavement design and PMS data for LF project (Ong Spur) ...	63
Figure 5.10 Representative structures for NE pavements: a) PCC structure-1 st scenario, b) PCC structure-2 nd scenario, and c) non-PCC structure	64
Figure 5.11 PCC structure-1 st scenario: ME predicted service life for different AC mixtures a) predicted rut depth and b) predicted total reflective transverse cracking	66
Figure 5.12 PCC structure-1 st scenario: Criteria selection for IDEAL CT test based on ME approach.....	67
Figure 5.13 PCC structure-1 st scenario: ME predicted service life for different AC mixtures a) predicted rut depth and b) predicted total reflective transverse cracking	68
Figure 5.14 PCC structure-2 nd scenario: Criteria selection for IDEAL CT based on ME approach	70
Figure 5.15 Non-PCC structure: ME predicted service life for different AC mixtures a) predicted rut depth and b) predicted total fatigue cracking	71
Figure 6.1 <i>CTIndex</i> for LTA specimens aged using NCHRP, NCAT, and adjusted NCAT	74

Figure 6.2 Black-space diagram: G-R test results for different binders	77
Figure 6.3 The G-R parameter for extracted binders obtained from different LTA protocols	78
Figure 6.4 The G-R parameter for extracted binders obtained from different LTA protocols	79
Figure 6.5 Various conditioning times for NCAT protocol: a) time vs. G-R parameter and b) time vs. IC=O parameters	80

List of Tables

Table 3.1 Information associated with different pavement projects.....	14
Table 3.2 Detailed information on performance tests and LTA protocols	23
Table 4.1 Ranking based on rutting resistance indices.....	29
Table 4.2 Overall evaluation of rutting resistance indices.....	30
Table 4.3 Tukey's HSD test results for cracking indices.....	35
Table 4.4 Ranking based on cracking resistance indices	36
Table 4.5 Summary of practical applicability of different performance-based tests.....	44
Table 5.1 Rating scale for pavement condition [66].....	54
Table 5.2 Rheological properties of asphalt binders in each project using DSR test	58

Acknowledgments

The authors would like to thank the Nebraska Department of Transportation (NDOT) for the financial support needed to complete this study. In particular, the authors thank NDOT Technical Advisory Committee (TAC) for their technical support and invaluable discussions/comments.

Abstract

This study aimed to propose a performance-based framework to evaluate highly recycled asphalt mixtures containing polymer-modified binders for potential use in a balanced mix design (BMD) specification in the state of Nebraska. For that, loose and compacted mixtures were directly collected from plant and field projects within a benchmarking study, subjected to an extensive experimental program. The laboratory investigation employed different monotonic tests recommended in BMD Phase 1, as well as the dynamic modulus test. Three long-term aging protocols were investigated in terms of their impact on the mechanical, rheological, and chemical characteristics of asphalt mixtures and binders. Moreover, field assessments with cores and pavement management system data were added to the analysis.

Results evaluated the sensitivity and significance of various tests for characterizing rutting and cracking resistance across mixtures varying in binder sources, grades, recycled contents, and warm mix additives. The variability and discrimination potential of performance-based parameters were identified, and suitable performance tests were suggested for the BMD framework considering the type of mixtures and site conditions of this study. The preliminary threshold criteria for each performance test were selected using a mechanistic-empirical approach considering three representative structural layers. Regarding the aging protocol, while the studied aging protocols yielded similar cracking resistance trends, their aging severity differed. Considering mechanical, chemical, and rheological similarities, an adjusted long-term aging protocol was selected for potential implementation in the state's BMD framework. Reheating and dwelling time impacted performance indices, showing they could be considered in criteria selection. The selected performance-based parameters and threshold criteria corroborated with the results from field rutting, roughness, and cracking assessments, which further verify the outcomes.

It was recommended to validate the selected performance tests, associated preliminary criteria, and aging protocol using more extended field data collection.

Chapter 1 Introduction

Transportation infrastructure, particularly roadways, plays a pivotal role in modern mobility systems, facilitating the efficient movement of people, goods, and services. Asphalt mixtures have been developed and refined to meet the demand for more durable and resilient pavement structures. The primary objective in asphalt mix design is to achieve an economically viable combination of materials (asphalt binder, aggregate, recycled material, additive, etc) that yields a composite material with adequate performance and durability. This balanced composition is crucial for the pavement's ability to multiple distresses when subjected to traffic loads and environmental conditions [1].

Although studies in asphalt mix design started in mid-1920 with Hubbard Field and continued with Hveem mix design in 1927 [2-4], the first widely adopted mix design system was called the Marshal method. The core principles of Marshall mix design method involved determining the optimal asphalt binder content based on stability and flow parameters, while concurrently considering key volumetric criteria such as air voids (AV), voids filled with asphalt (VFA), and voids in the mineral aggregates (VMA). However, this method exhibited several limitations, primarily associated with the sample compaction process and the selection criteria for aggregate gradation and binder content. Moreover, the method failed to account for climate and region-specific factors in mixture design. Additionally, the Marshall mix design method placed insufficient emphasis on aggregate gradation design, which subsequently contributed to premature rutting and raveling in asphalt pavements [3-4].

In 1993, the Strategic Highway Research Program (SHRP) introduced the Superpave mix design, with the primary objective of developing a mix design procedure that could account for varying weather and traffic conditions across the United States. To achieve this, the Superpave

mix design incorporated the Superpave Gyrotory Compactor (SGC), which more closely simulates field compaction than traditional impact compaction methods used for sample fabrication. Additionally, it included performance evaluation of asphalt concrete. This method was structured into three levels of increasing complexity (Level 1, Level 2, and Level 3) [5]. The currently employed mix design practice (Level 1) implements traffic-based material design and incorporates an advanced asphalt binder selection process tailored to diverse climatic conditions. The Level 1 Superpave mix design primarily involves proportioning asphalt binder and aggregates, taking into account empirical aggregate properties and volumetric characteristics including VMA, VFA, AV, and specific gravity. Further, SHRP introduced a new classification system for asphalt binders in the early 1990s, known as Performance Grading (PG). While Levels 2 and 3 incorporated performance-based specifications and developed several procedures for predicting and evaluating mixture performance, these advanced levels were not implemented by any state Departments of Transportation (DOTs).

The Superpave Level 1 procedure has been subjected to criticism from state DOTs and asphalt contractors, primarily due to its perceived inability to accurately predict the long-term performance of asphalt mixtures. The limitations of this method stem from its inadequate accuracy and overreliance on volumetric characteristics of asphalt mixtures [6]. For instance, while specific requirements were established for volumetric properties during the design process, their calculation was heavily dependent on aggregate specific gravity measurements, which are prone to accuracy issues. Numerous reports have documented significant problems with accuracy and variability in specific gravity measurements [7]. Furthermore, the incorporation of reclaimed asphalt pavement (RAP) [8-10], along with additive modifications such as adding different types of recycling agents [9, 11-12], antioxidants [13], polymers [14], and fibers [15] further complicated

the application of this method and potentially reduced its accuracy. Specifically, the introduction of these new technologies can significantly affect asphalt mixture performance in ways that volumetric mixture design methods are incapable of fully capturing. Consequently, two mixtures with nearly identical volumetric characteristics may exhibit markedly different performance in terms of rutting or cracking properties [16].

To address these issues, the Balanced Mix Design (BMD) was proposed, aiming to evaluate the performance of asphalt mixtures during the design phase. In the BMD approach, the selection of materials and mix proportions are determined considering not only the asphalt concrete (AC) volumetric parameters but also its response to different testing conditions that lead to various distress modes such as fatigue cracking, rutting, moisture damage, low temperature cracking, etc. The analysis of performance-based indices of various ACs produced with alternative and conventional materials can lead to optimum blends while obtaining satisfying performances. The ultimate goal is to optimize the asphalt mixture while balancing the performance against major distresses that occur on asphalt concrete in the field. Identification of the main pavement distresses and the associated testing methods to address them are the key features in the BMD concept. Nowadays, great efforts are ongoing in various state DOTs to incorporate BMD methodology [17-27]. The incorporation of any mixture performance test into the BMD procedure necessitates the establishment of criteria for test results. These criteria must be founded on a robust correlation with field performance and tailored to the specific mixtures employed in a particular state or region.

A survey of state DOTs and transportation agencies was performed under project NCHRP 20-07/Task 406 [28] which identified rutting, cracking (Fatigue, thermal, and reflection), and moisture damage as the main distress types that need to be addressed within performance testing.

AASHTO PP 105-20 delineates four distinct Balanced Mix Design (BMD) approaches for asphalt mixture design: A) volumetric design with performance verification, B) volumetric design with performance optimization, C) performance-modified volumetric design, and D) performance design. All BMD approaches mandate that designers verify and meet performance-based properties of the end product, rather than solely relying on volumetric properties. This end-product testing paradigm not only facilitates greater innovation in material selection but also provides agencies with a more reliable methodology for accepting mixtures for specific pavement applications. More details about BMD and different approaches could be found elsewhere (BMD Phase 1 report). Consequently, it is imperative for all state DOTs to develop a comprehensive understanding of the most appropriate performance-related tests in terms of reliability, repeatability, and simplicity, as well as to identify the most suitable approach for implementing the BMD methodology.

Regarding AC mid-temperature cracking, several tests are recommended in the BMD, such as Direct Tension Cyclic Fatigue Test, Flexural Bending Beam Fatigue (BBF) Test, Illinois Flexibility Index Test (I-FIT), Indirect Tensile Cracking Test (IDEAL-CT), Overlay Test (OT), and Semi-Circular Bend (SCB) Test [1], [19], [21], [29], [30]. Several efforts are ongoing to establish and implement reliable performance tests for laboratory evaluation of mid-temperature cracking in asphalt mixtures. The Illinois and Oregon DOTs recommended the IFIT to characterize cracking performance, while three days and one day of oven aging at 95°C is selected for the long-term aging (LTA) conditioning, respectively [31]. The California DOT has included the BBF test along with the mechanistical empirical pavement design program in its BMD framework [21]. Texas and New Jersey DOTs adopted OT for both design and production phases. Further, IDEAL-CT was recently selected by Texas, New Jersey and Virginia DOTs as a simple

and rapid test to characterize mid-temperature cracking [30]. Texas DOT recommends a correlation between the OT and IDEAL-CT during the job mix formula (JMF) determination and the further use of IDEAL-CT during QC/QA phases [26], [32]. Louisiana DOT selected the SCB test for cracking assessment as they develop an accelerated aging protocol and are also implementing SCB into QC/QA phases [22], [33].

A number of performance tests, including Hamburg wheel track test (HWTT), Repeated Simple Shear Test (RSST), Asphalt Pavement Analyzer (APA), High-temperature IDT, and Indirect Tensile Rutting Test (IDEAL-RT) are being used in different BMD frameworks to determine rutting resistance. Illinois, California, Iowa, Texas, Louisiana, and Oregon DOTs have adopted HWTT for the evaluation of their asphalt mixtures, while New Jersey and Virginia DOTs selected APA in their BMD framework [8], [19], [20]. High-temperature IDT and IDEAL-RT are also considered as simple and rapid tests in many recent investigations to be used for rutting assessment in BMD [30].

Implemented BMD protocols vary considerably between states. This variation can be attributed to several factors, including but not limited to the diversity of equipment available in laboratories around the country, the knowledge and experience levels of technicians with different testing methods, the specific materials commonly used within a state, and the site location and climatic conditions of the region. It is imperative that region-specific efforts are undertaken to account for the scenarios and conditions encountered by each state. Each state must identify appropriate tests that exhibit sensitivity to the materials and procedures commonly employed within that state, as well as establish specific threshold values that satisfy the state's quality criteria.

In Nebraska (NE), RAP is utilized in 25 to 45% of the mixture, with a target of 65% for future applications. Additionally, various WMA additives are incorporated into polymer-modified binders, mainly functioning as a compaction aid. Furthermore, NE encompasses diverse climatic zones, with an overall temperature range spanning from -40 to 40 °C. The state is putting efforts into developing a BMD protocol, with initial investigations focused on identifying the most suitable mid-temperature cracking and rutting tests. Initial studies in 2019 suggested SCB and Gyratory stability tests as appropriate for NE BMD implementation [6]. However, with recent advancements in BMD, the importance of benchmarking studies using a wide range of asphalt mixtures commonly employed within the region has become evident. Further, developing a BMD framework without considering various performance tests and associated criteria, long-term aging effects, and field data analysis would lack sufficient reliability. As such, the Nebraska BMD project was started in 2022 with Phase 1 mostly focused on different simple static performance tests [4]. The results from Nebraska BMD Phase 1 led to determining IDEAL-CT and IDEAL-RT as two simple performance tests that could appropriately characterize mid-temperature cracking and rutting of Nebraska mixtures, respectively [4]. However, these simple surrogate tests are only reliably accurate when finding a correlation with fundamental materials properties. Furthermore, the application of the performance tests in a BMD framework requires specifying threshold/criteria, as well as defining appropriate and practical long-term aging procedures which can only be derived through long-term benchmarking studies along with field data collection. With that in mind, there is a certain need for new research to identify performance testing protocols that exhibit sensitivity in discriminating between various NE asphalt mixtures by capturing their mechanical responses while remaining practical for implementation within the state's BMD framework.

1.1 Research Objectives

The primary objective of this study was to develop a performance-based framework that could efficiently evaluate the performance of high-content RAP-recycled asphalt mixtures produced with polymer modified asphalt binders in the state of Nebraska. For that, it was critical to assess the sensitivity of several mixtures to various performance tests. Furthermore, the initial threshold criteria for each test needed to be identified, as well as an appropriate LTA protocol. To achieve these objectives, a comprehensive dataset derived from both laboratory and field investigation, coupled with statistical analyses and mechanistic-empirical pavement design approaches was employed. The results from the BMD Phase 1 project were utilized to find the most appropriate and practical performance tests, as potential tests to be used in the Nebraska BMD framework. With respect to the research plan illustrated in Figure 1.1, the study can be divided into three steps:

1.1.1 Step 1: Laboratory Assessment of NE Mixtures Using Different Performance Tests

Considering the potential effects on performance test results, a diverse selection of six plant-produced asphalt mixtures with various binder sources and grades, different binder and RAP contents, and different warm additives were employed in this study. A set of simple monotonic performance tests (detailed in Section 3.2) selected from Phase 1 of this study were conducted on plant-produced laboratory-compacted specimens. The indices obtained from the selected tests were evaluated in terms of results variability, discrimination potential between different mixture compositions, ranking of asphalt mixtures performance, and correlation among various indices. For the evaluation of cracking resistance, along with the short-term aged (STA) samples, three different mechanisms for laboratory long-term aging (LTA) conditioning were also considered. Finally, the Dynamic Modulus (DM) test was conducted to determine the linear viscoelastic (LVE)

properties of the mixtures, E^* and Glove-Rowe parameters, to estimate their rutting and cracking potential, and further used to validate the findings from the simple static performance tests.

1.1.2 Step 2: Validation of Performance Test Results Based on Field Assessment

In this second step, the performance test parameter(s) that exhibited higher correlation with fundamental test parameters, as well as greater sensitivity to materials in laboratory compacted asphalt mixtures, were selected for further assessment. Field core samples and PMS data (IRI, rutting depth, and cracking percentage) were collected within a specific time frame at the same reference points for all projects under consideration. With that, step 2 enabled the determination of the variability of test results derived from field core samples, the effect of the reheating process on performance indicators, the compatibility of test results with actual pavement conditions, and the establishment of preliminary threshold values for the performance parameters.

1.1.3 Step 3: Selecting Preliminary Threshold Criteria and Appropriate LTA Protocol

In the third step of the study, three LTA protocols were applied to find the appropriate and accurate aging protocol to be used in the BMD framework. The NCHRP 09-54 method, the critical aging method (NCAT), and an adjusted critical aging method were utilized for this purpose (details in Section 3.2.6). To this end, the mechanical, rheological, and chemical characterization of asphalt mixtures and recovered binders aged under different LTA protocols was conducted. With that, the adjusted aging procedure that could simulate the results of the well-established LTA protocol was determined but remains to be practical for a BMD framework. To determine the preliminary threshold criteria for the selected performance tests, a mechanistic-empirical approach was adopted. In this method the service life of pavements was predicted for different asphalt mixture layers (with the same structural layers underneath) and the predicted service life was compared to the performance tests' indices to define the initial threshold criteria for each performance test.

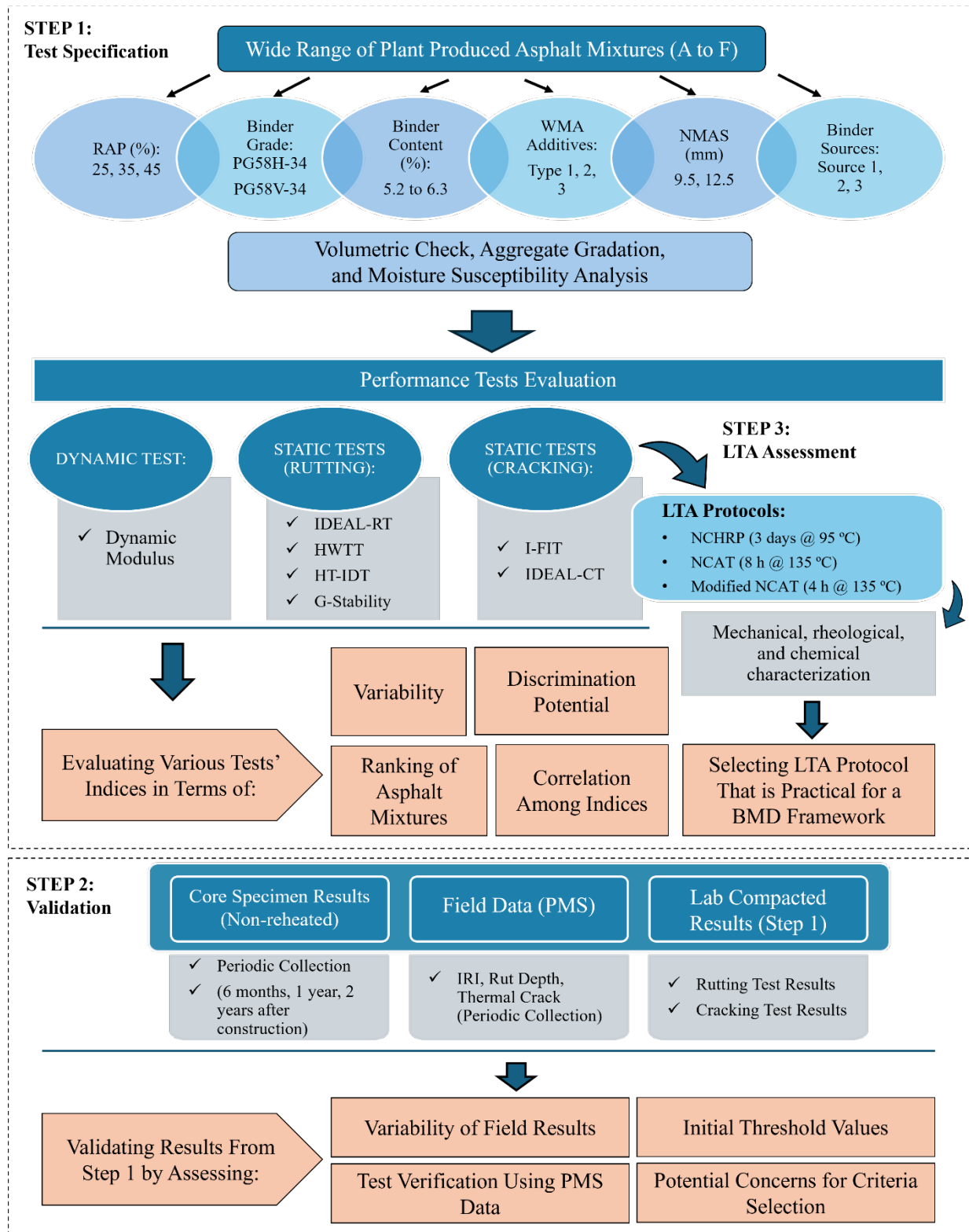


Figure 1.1 Experimental plan adopted in this study.

1.2 Organization of the Report

This report is structured into six chapters. Chapter 1 introduces the history of asphalt mix design and the rationale for developing the BMD framework. It presents a comprehensive literature review of various states' practices in implementing BMD, followed by an examination of efforts undertaken in Nebraska. This chapter also elaborates the research gaps that need to be addressed for Nebraska's BMD implementation. Subsequently, Chapter 2 provides a summary of BMD Phase 1. Chapter 3 represents research methodology, focusing on the materials, experimental methods, field evaluation, and protocol establishment. Chapter 4 presents laboratory and field test results, accompanied by statistical analyses to determine the appropriate performance tests for Nebraska BMD. Chapter 5 represents the mechanistic-empirical approach that was adopted to determine the preliminary threshold criteria for each performance test. Chapter 6 shows the adopted method for determining appropriate and practical LTA protocol using mechanical, chemical, and rheological characteristics of asphalt mixtures and binders. Finally, Chapter 7 summarizes findings and conclusions derived from this research project.

Chapter 2 Summary of Nebraska BMD Phase 1 Project

In Phase 1 of this project, the Nebraska Department of Transportation (NDOT) initiated a study to investigate the feasibility of implementing a BMD approach for asphalt mixtures in the state. The study focused on evaluating various performance tests to address rutting, fatigue cracking, and moisture damage in asphalt pavements. The primary objectives were to evaluate and select appropriate performance tests to be used in the Nebraska BMD framework. The study examined several performance tests on common Nebraska asphalt mixtures, including the Hamburg wheel tracking test (HWTT), indirect tensile asphalt rutting test (IDEAL-RT), high temperature indirect tensile test (HT-IDT), and Gyratory stability test (G-stability) for rutting resistance. Fatigue cracking resistance was assessed using the Illinois flexibility index test (I-FIT) and indirect tensile asphalt cracking test (IDEAL-CT). Moisture damage resistance was evaluated using the tensile strength ratio (TSR), HWTT, HT-IDT, and G-stability tests. These tests were conducted on a limited number of both plant-mixed laboratory-compacted (PMLC) specimens and field cores taken at 6- and 12-months post-construction. Additionally, long-term aging protocols (NCHRP 09-54 and NCAT) were evaluated for the fatigue cracking tests.

Key findings from the rutting tests revealed that while the HWTT is well-established, its cost and time requirements make it impractical for production and quality control testing. The IDEAL-RT test showed the highest correlation with HWTT results, followed by HT-IDT and G-stability. Based on these results, and considering the cost effectiveness of IDEAL-RT, this test was recommended as a good candidate for BMD implementation, although it was clarified that more field data is needed for further validation of the findings. For fatigue cracking tests, the I-FIT showed higher result variability, likely due to the more complex sample preparation procedure. The IDEAL-CT correlated well with I-FIT, especially for long-term aged specimens. Given its

simplicity and lower variability, IDEAL-CT was recommended as a potential replacement or complement to I-FIT in the BMD framework. Moisture damage test results showed no strong correlations between tests, except for some similarity between G-stability and TSR rankings. This suggests that more investigation is needed on surrogate tests and conditioning protocols for moisture damage assessment.

The study also compared long-term aging protocols, including NCHRP 09-54 which is an established method that takes a long time (five days) in the lab to simulate long-term aging, and NCAT protocol which is more recently developed with the potential of simulating mixtures' long-term aging in eight hours. Findings showed that the NCAT protocol caused more severe aging than NCHRP 09-54 with both methods resembling similar trends in terms of cracking test results. However, it was specified that long-term field data as well as rheological and chemical binder test analyses are needed to validate these aging protocols and their correlation to real-world pavement aging.

The Phase I study represented the first step in developing a comprehensive BMD framework for Nebraska. While this study provided an initial understanding of acceptable parameter values based on historical mixtures' performances, more field data during pavement service life is needed to establish trusted threshold values. Future recommendations included continuing annual field data collection, verifying the sensitivity of selected performance tests to the mixture constituents using fundamental mechanical tests, further evaluating long-term aging protocols, conducting rheological and chemical characterization of aged binders, expanding the study to a wider range of mixtures and conditions, and developing correction factors for non-standard geometries in certain tests.

Chapter 3 Site Location, Materials, and Test Methods

This chapter details the materials, testing methodologies, and performance evaluation procedures adopted in this research. Additionally, it provides comprehensive documentation of sampling locations for loose asphalt mixtures and field cores, along with protocols for field condition monitoring.

3.1 Materials, Projects, and Site Locations

A varied range of commonly used NE asphalt mixtures from six different projects were selected for this study (four projects were continued from Phase 1 of the study). The collected mixtures were transferred to the laboratory for further evaluation. The specimens compacted in the laboratory are denoted as LX, with "L" representing laboratory, and "X" representing project IDs (X=A to F). Core specimens extracted from pavements are labeled as CX, with "C" indicating core samples. Field data from the pavement management system for various specimens are designated as FX, where "F" signifies field data. As the short-term aging (STA) procedure had been implemented in the plant, a two-hour conditioning period at the compaction temperature was adopted prior to specimen fabricating in the laboratory. To simulate long-term aging, NCHRP 09-54 and critical aging (referred to as NCAT) protocols were applied on the loose asphalt mixtures [34], [35]. The primary Superpave mix design criteria including aggregate gradation requirements, dust to binder ratio, and moisture susceptibility were assessed on the mixtures, with the results indicated in Table 3.1 and Figure 3.1 [36]. Considering performance grade (PG) test results, the high-temperature PG of all mixtures was defined to be PG-64-XX.

Table 3.1 also provides additional mixture characteristics, showing the diverse selection of projects. The mixtures were categorized into SPR and SLX types, incorporating RAP contents ranging from 25% to 45% and utilizing three different WMA additives at 0.7% by binder weight:

Evotherm®, Delta S®, and AD-here® ULTRA. Evotherm® functions as a compaction aid by reducing binder viscosity, enabling lower mixing and compaction temperatures. Delta S® serves as both a rejuvenator and WMA technology, designed to restore aged binder functionality by reversing oxidation while reducing production temperatures. AD-here® ULTRA was developed to facilitate lower temperature production while enhancing mixture resistance to moisture damage. The mixtures were designed with nominal maximum aggregate size (NMAS) of either 9.5 or 12.5 mm, utilizing blends of gravel and limestone aggregates. The aggregate gradations for different mixtures are presented in Figure 3.1.

Table 3.1 Information associated with different pavement projects.

Mix ID	A	B	C	D	E	F
Mix Type/Location	SLX/Crofton	SLX/I-480	SPR/Gresham	SPR/Tekamah	SLX/Grand Island	SPR/Ong Spur
Binder Source/Grade	J/PG 58H-34	FH/PG 58V-34	FH/PG 58H-34	M/PG 58H-34	FH/PG 58H-34	FH/PG 58H-34
RAP (%)	35	25	45	45	35	45
WMA Additive	Evotherm®	Delta S®	AD-here®	Delta S®	AD-here®	AD-here®
Binder Content (%)	6.3	5.3	5.2	5.4	5.5	5.5
NMAS (mm)	9.5	9.5	12.5	12.5	9.5	12.5
Maximum Specific Gravity(G_{mm})	2.41	2.45	2.39	2.45	2.41	2.42
Dust/Binder Ratio	1.03	1.21	1.22	1.23	1.04	0.77
Tensile Strength Ratio (%)	94.4	83.3	89	83.1	84	86.2

Note: J: Jebro, FH: Flint Hills, M: Monarch

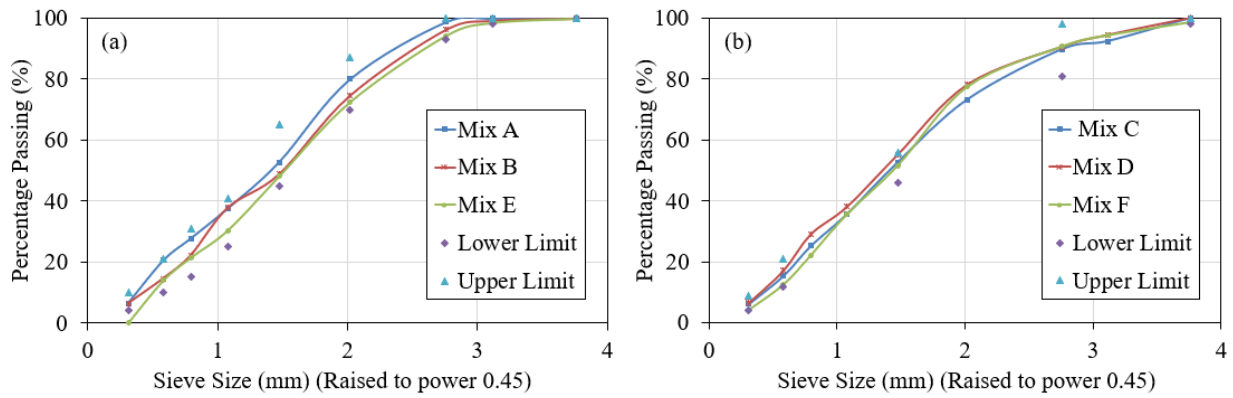


Figure 3.1 Aggregate gradation and criteria (a) mix A, B, E and (b) mix C, D, F

Six asphalt mixtures (three SLX and three SPR) were collected from northern and southern Nebraska to account for potential climatic effects on pavement performance. The sampling locations of different projects are illustrated in Figure 3.2.

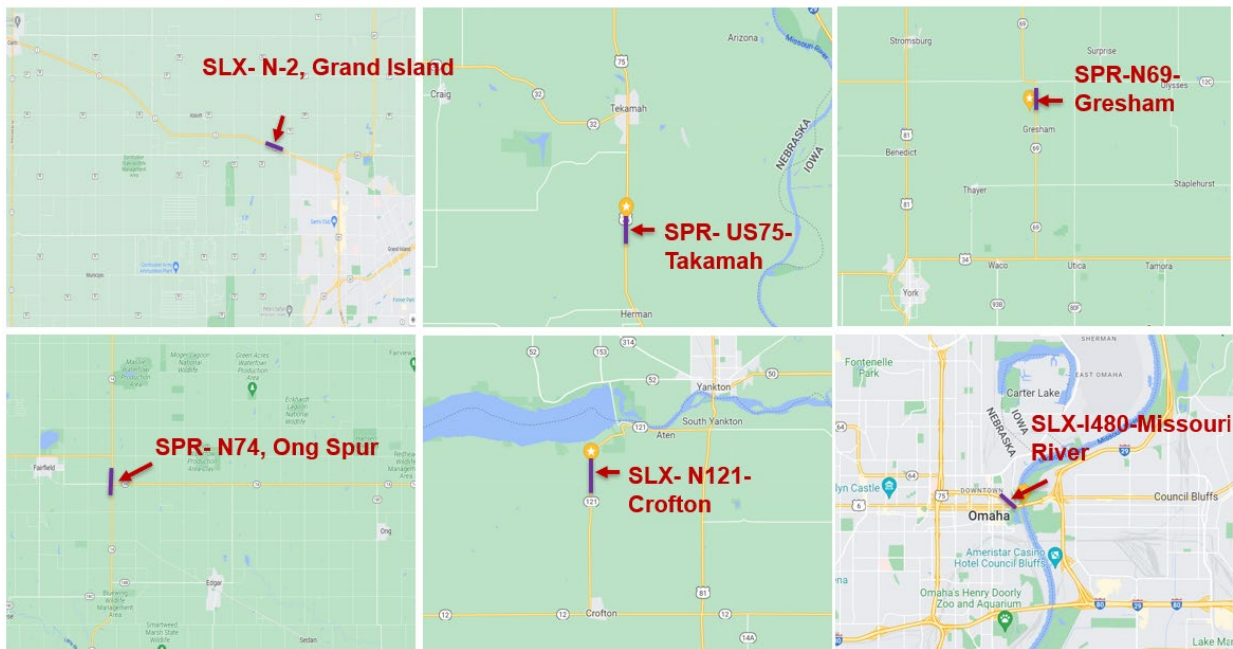


Figure 3.2 Site location of the selected projects in this study

3.2 Performance Test Methods and Aging Protocols

3.2.1 Dynamic Modulus (DM) Test

The DM test was performed following AASHTO T 378 standard, in which cylindrical specimens (100-mm diameter by 150-mm tall with $7 \pm 0.5\%$ air void) were subjected to a controlled sinusoidal compressive stress maintaining axial strain between 75 to 125 microstrain for unconfined conditions. The test was run at three different temperatures (4, 21, and 40 °C) and ten different frequencies (from 0.01 to 25 Hz). Figure 3.3 illustrates the test setup associated with the DM test. The dynamic modulus ($|E^*|$) is the main parameter derived from this test which is a performance-related property that can be used for characterizing the mixtures' stiffness in the linear viscoelastic region. Additionally, the phase angel (δ), representing the lag between applied stress and resulting strain, was measured to evaluate the time-dependent deformation characteristics under various temperatures and loading frequencies. To evaluate the DM test results, the Arrhenius equation was used within the time-temperature superposition principles to generate master curves for each mixture [37, 38]. This equation correlates the shift factor (α_T) with temperature, allowing the data collected at various temperatures to be shifted along the frequency axis to form a continuous master curve. The Arrhenius time-temperature superposition model for computing α_T is expressed in Equation 3.1 [38]:

$$\text{Log}(\alpha_T) = C_a \left(\frac{1}{T_i} - \frac{1}{T_{ref}} \right) \quad (3.1)$$

Where C_a is the material constant that is a function of the activation energy; T_i is the test temperature of interest; and T_{ref} is the reference temperature of interest.

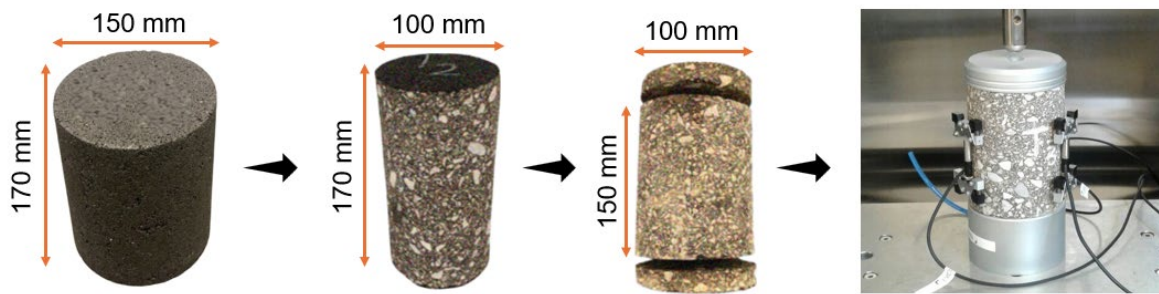


Figure 3.3 DM test setup and sample preparation

3.2.2 Hamburg Wheel Tracking Test (HWTT)

The HWTT was performed on laboratory compacted and field core specimens following AASHTO T 324. The test subjected cylindrical specimens to a 705 N steel wheel load at 50 °C until reaching failure rutting depth or 20,000 passes. Laboratory specimens (62 ± 1 mm thickness, $7 \pm 0.5\%$ air void) were prepared using a Superpave Gyratory Compactor (SGC), while field cores (around 50 mm thickness) were modified with a mix capping compound to achieve the required 62 ± 1 mm height. Figure 3.4 shows the HWTT setup along with sample preparation.

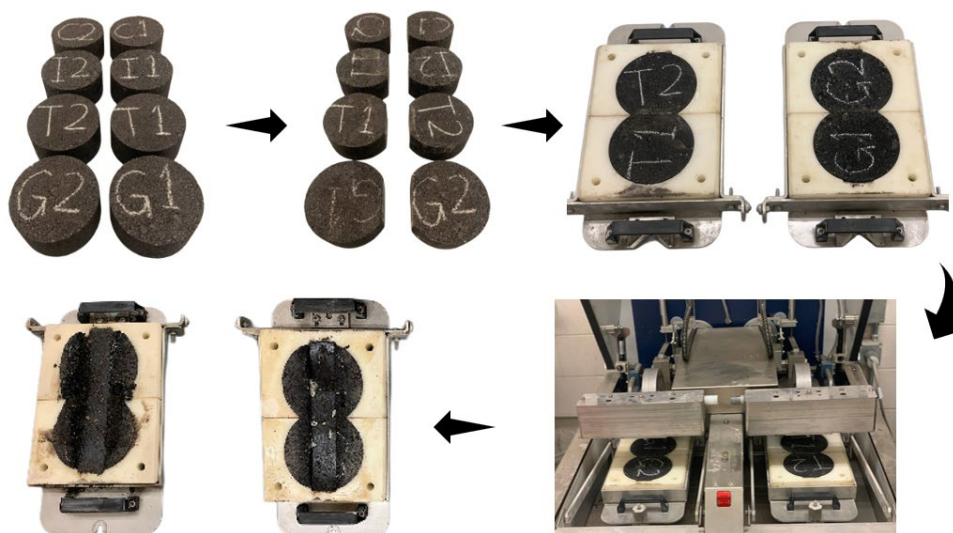


Figure 3.4 HWTT setup and sample preparation

3.2.3 Indirect Tensile Asphalt Rutting Test (IDEAL-RT)

The IDEAL-RT (ASTM standard under preparation) was conducted on cylindrical specimens with a diameter of 150 ± 2 mm and a height of 62 ± 1 mm, at 50°C with a loading rate of 50 ± 2.0 mm/min [26]. The load and Load-Line Displacement (LLD) were recorded during the test to determine the maximum shear strength and rutting tolerance index (RT_{Index}). Filed core specimens followed the same procedure, only the specimens normally had a height of around 50 mm, conforming to the required thickness of 38 to 95 mm [26]. Figure 3.5 indicates the IDEAL-RT setup used in this research study. The RT_{Index} was calculated using Equation 3.2:

$$RT_{Index} = 2.356E - 5 \times \frac{P_{max}}{t \times w} \quad (3.2)$$

Where RT_{Index} is the rutting tolerance index, P_{max} is the maximum load (N), t is the specimen thickness (m), and w is the width of the upper loading strip ($=0.0191$ m).

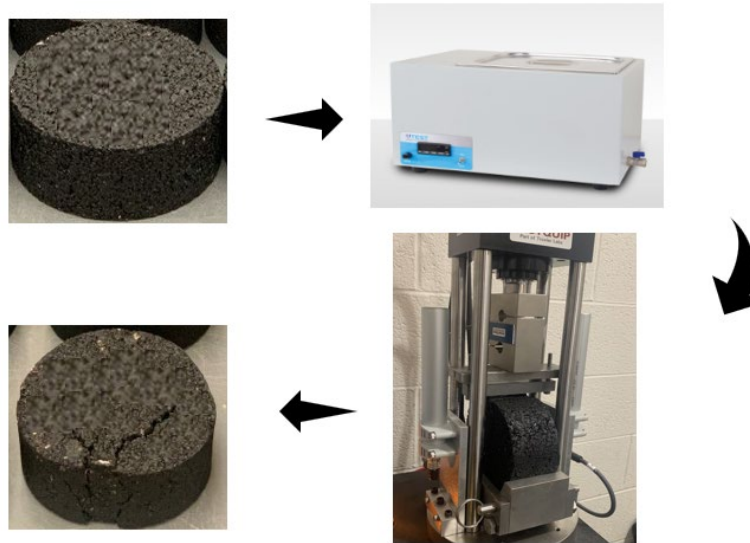


Figure 3.5 IDEAL-RT test setup and sample conditioning

3.2.4 Illinois Flexibility Index Test (IFIT)

The IFIT was conducted in accordance with AASHTO T 393 standard. Following the protocol, semi-circular specimens with dimensions of 150 mm in diameter and 50 mm in thickness were cut, notched, and placed in the test fixture. The samples were subjected to loading along the vertical radius (at 50 mm/min) while maintaining a testing temperature of 25 ± 0.5 °C. Throughout the testing procedure, both load and load line displacement (LLD) measurements were recorded to determine the fracture energy (G_f) and post peak slope ($|m|$), enabling the calculation of the flexibility index (FI) as a cracking resistance indicator for AC mixtures. Figure 3.6 shows the IFIT test setup and sample preparation procedure. For field evaluation purposes, core specimens ranging from 25 to 50 ± 1 mm in thickness were deemed acceptable; thus, core specimens measuring around 38 mm in height were used, with their test results adjusted using a thickness correction factor. To determine the $|m|$, a tangential curve was drawn at the inflection point, with its slope representing the $|m|$ value. The FI can be calculated by Equation 3.3:

$$FI = \frac{t}{50} \times \frac{G_f}{|m|} \times A \quad (3.3)$$

Where G_f is the fracture energy (J/m^2), $|m|$ is the absolute value of the post-peak load slope (KN/mm), A is a unit conversion and scaling factor equal to 0.01, and t is the average specimen thickness (mm).

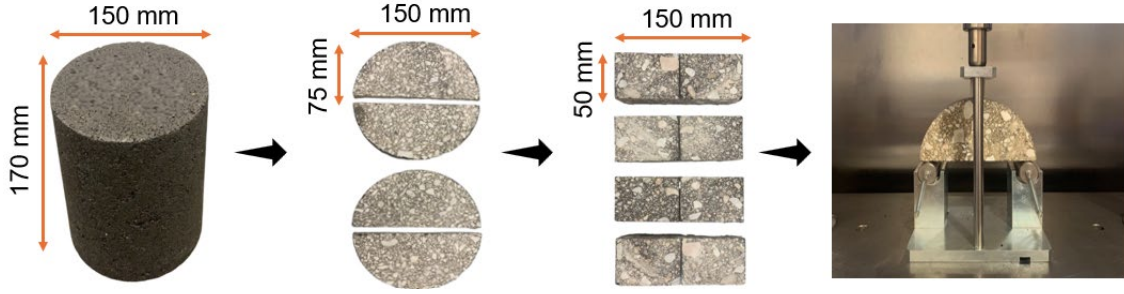


Figure 3.6 IFIT setup and sample preparation procedure

3.2.5 Indirect Tensile Asphalt Cracking Test (IDEAL-CT)

The IDEAL-CT was conducted in accordance with ASTM D 8225 standard. The testing procedure involved preparation of cylindrical specimens measuring 150 mm in diameter and 62 mm in height, with 7 ± 0.5 percent air void content. The testing was performed at 25 ± 0.5 °C using a load point displacement (LPD) mechanism at a rate of 50 mm/min, from which the cracking tolerance index (CT_{Index}) was derived as the primary performance-related cracking parameter. Field evaluation protocols allowed the use of core specimens of varying thicknesses (38, 50, 62, 75 mm), with a correction factor needed in the formula. Figure 3.7 indicates IDEAL-CT setup and sample preparation. The CT_{Index} was calculated using Equation 3.4. The justification for selecting the critical point at 75% of the peak load in the post-peak region has been detailed elsewhere [39].

$$CT_{Index} = \frac{t}{62} \times \frac{G_f}{m_{75}} \times \frac{l_{75}}{D} \quad (3.4)$$

Where G_f is the fracture energy (J/m^2), m_{75} is the interval slope of load-displacement curve between 65% and 85% of the peak load, and l_{75} is a “strain” tolerance parameter when the load reduced to 75% of the peak load.

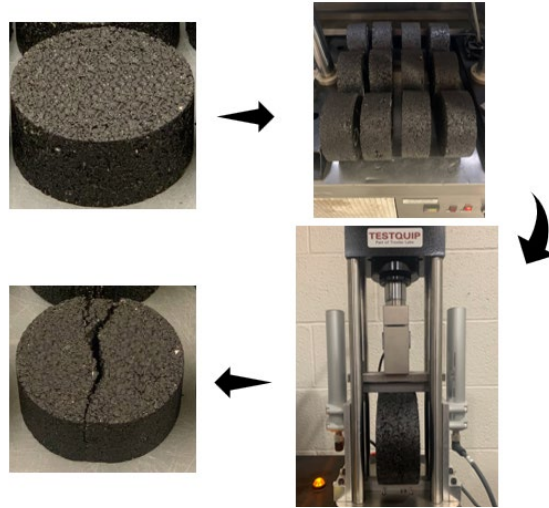


Figure 3.7 IDEAL-CT setup and sample geometry before and after running the test








3.2.6 Short-term Aging (STA) and Long-term Aging (LTA) Protocols

Given the established understanding of how aging affects the mechanical performance of asphalt mixtures, various laboratory aging protocols have been developed to simulate STA and LTA during the design and production phases [4]. As for the materials in this study, loose asphalt mixtures were collected directly from project sites, a short-term aging procedure was not required. Consequently, only two hours of conditioning at the compaction temperature was applied prior to specimens' fabrication.

To simulate LTA in the lab, two common protocols were applied: the National Cooperative Highway Research Program (NCHRP) 09-54 protocol and the National Center for Asphalt Technology (NCAT) protocol (also referred to as critical aging method). The NCHRP 09-54 protocol involved aging the loose mixture at 95 °C for three days, which simulates eight years of field aging at 20 mm below the pavement surface in Nebraska conditions [40]. Although this is a well-established protocol to simulate LTA in the field, it is time consuming and impractical for implementation during the production phase within a BMD framework. The alternative NCAT

protocol employed in this study applied eight hours of conditioning at 135 °C on the loose asphalt mixtures to simulate LTA. In this study, specimens conditioned using both aging protocols were subsequently used in fatigue cracking test analyses. With the results derived from cracking tests (detailed in Section 4.1.3), a third LTA protocol, named adjusted NCAT, was also implemented on the mixtures which involved conditioning loose asphalt mixtures at 135 °C for four hours. Table 3.2 summarizes information on different performance tests and LTA protocols applied in this study.

Table 3.2 Detailed information on performance tests and LTA protocols

Test (Standard)	Temperature/ Loading Conditions	Parameter Equation	and/or	Parameter's Definition	Setup
DM (AASHTO T 378)	4, 21, 40 °C / Test Frequencies: 0.01 to 25 Hz	$ E^* $ and δ master curves at 21 °C $ E^* $ at 38 °C and 0.1 Hz $G - Rm = \frac{ E^* \times (\cos \delta)^2}{\sin \delta}$		$ E^* $: dynamic modulus δ : phase angle $G - Rm$: Glover-Rowe parameter	
HWTT (AASHTO T 324)	50 °C / Applied Force: 705 ± 4.5 N Load rate: 52 ± 2 passes/min	Rut depth		Rutting depth (mm) at 7,500 load cycles	
IDEAL-RT (ASTM under preparation)	50 °C / Load rate: 50 ± 2.0 mm/min	RT_{Index} $= 2.356E - 5 \times \frac{P_{max}}{t \times w}$		P_{max} : max load (N) t : sample thickness (m) w : width of the upper loading strip (0.0191 m)	
HT-IDT (ALDOT-458)	50 ± 1 °C / Load rate: 50 mm/min	$HT - IDT = \frac{2 \times P_{max}}{\pi \times D \times H}$		P_{max} : max. load (kN) D : average diameter (mm) H : height (mm).	
G-stability (Nsengiyum va et al., 2020)	54 °C / Load rate: 50 ± 2.0 mm/min	$Rut\ Index = \frac{G-stability}{G-flow}$		G-stability: Peak load (kN) G-flow: Displacement (mm)	
3.3I-FIT (AASHTO - T 393)	25 ± 0.5 °C / Load rate: 50 mm/min	$FI = \frac{t}{50} \times \frac{G_f}{ m } \times A$		G_f : fracture energy (J/m ²), m : post-peak slope(kN/mm) t : sample thickness (mm) A : unit factor 0.01	
IDEAL-CT (ASTM D 8225)	25 ± 0.5 °C / Load rate: 50 mm/min	$CT_{Index} = \frac{G_f}{ m_{75} } \times \frac{l_{75}}{D}$		G_f : fracture energy (J/m ²) m_{75} : post peak slope (N/m) l_{75} : After peak displacement at 75% of peak load (mm) D : diameter (mm)	
LTA Protocol	Temperature	Time		Sample condition	
NCHRP 09-54 (Kim et al., 2015)	95 °C	3 days (simulate 8 years of aging at 20 mm below surface)		Loose Mixture	
NCAT (Chen et al., 2018)	135 °C	8 hours		Loose Mixture	
Adjusted NCAT	135 °C	4 hours		Loose Mixture	

Chapter 4 Laboratory Test Results and Discussion

4.1 Step 1: Laboratory Assessment of NE Mixtures using Different Performance Tests

4.1.1 Dynamic Modulus Test Results

Following AASHTO T 378 standard, three replicates were tested for each mixture studied. The reliability of the results was confirmed through coefficient of variance (COV) of 6.13% and 4.83% for the $|E^*|$ and δ measurements, respectively. The time-temperature superposition principle (Equation 3.1) was applied to the averaged replicate data to construct $|E^*|$ and δ master curves at a reference temperature of 21 °C, as illustrated in Figure 4.1. As can be seen in Figure 4.1a, the master curves reveal that LD has the highest $|E^*|$ values at lower frequencies (corresponding to higher temperatures), where $|E^*|$ serves as an indicator of material stiffness. Higher $|E^*|$ values at high temperatures typically correlate with enhanced rutting resistance. Conversely, LA and LE show the lowest $|E^*|$ values at the low frequency ranges, suggesting inferior rutting resistance across the loading spectrum.

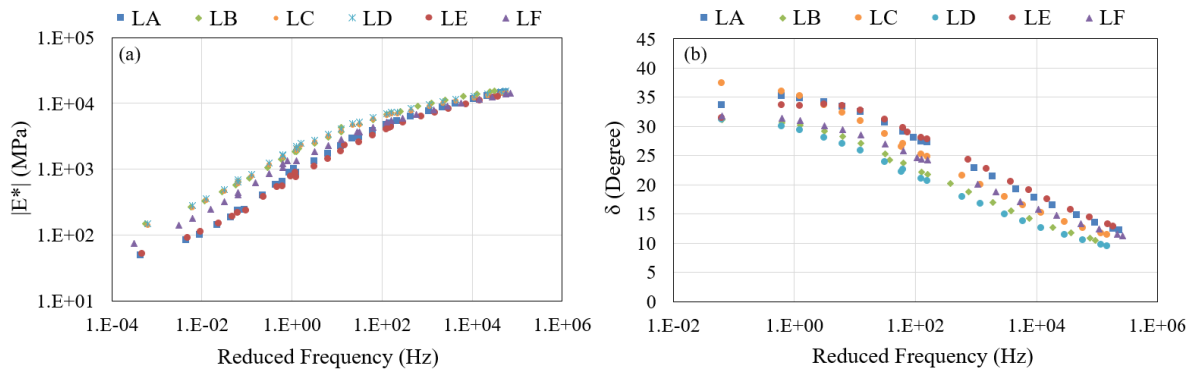


Figure 4.1 Master curves at 21 °C: (a) $|E^*|$ and (b) δ .

To further analyze rutting resistance potential of asphalt mixtures, the $|E^*|$ value measured at 38 °C and 0.1 Hz was selected, as this parameter has demonstrated strong correlation with rutting resistance derived from flow number test [20], [47]. Based on the results plotted in Figure 4.2a, LD has the highest $|E^*|$ value followed by LC and LB. These results can be explained by the synergistic effect of RAP content, binder type, and binder content. First, LD and LC have 45% RAP content with the lowest binder content. The stiff aged binder present in RAP materials and limited binder blending around RAP particles have been identified as an effective factor for this behavior [48], [49]. Despite having a lower RAP content, the high $|E^*|$ for LB mixture could be attributed to the use of a PG 58V-34, which offers superior rutting resistance compared to PG 58H-34 used in the other mixtures. The lowest $|E^*|$ values are for LA and LE which could be related to the higher binder content in their mix design compared to the other mixtures (6.3 and 5.5%, respectively).

Taking into account the cracking potential, a higher $|E^*|$ coupled with lower δ at higher frequencies (lower temperatures) is often associated with a reduced cracking resistance in asphalt mixtures. As can be seen in Figure 4.1a, while the $|E^*|$ values at high frequencies show a similar trend to those at lower frequency ranges; the numbers are closer to each other. Analysis of δ in Figure 4.1b reveals that LD and LB have the lowest phase angle which indicates reduced relaxation capability and increased cracking susceptibility of these mixtures. Alternatively, the Glover-Rowe ($G-R_m$) parameter for asphalt mixtures can be adopted as a performance index to indicate the propensity for crack initiation in asphalt mixtures [50], [51]. Lower values of the $G-R_m$ parameter are associated with higher cracking resistance. Figure 4.2b shows the $G-R_m$ results.

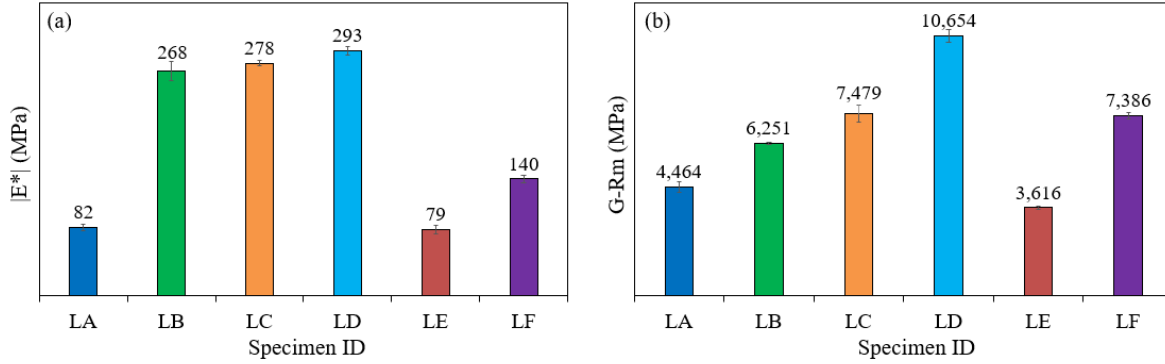


Figure 4.2 (a) $|E^*|$ value at 38 °C and 0.1 Hz, (b) G-R_m parameter at 20 °C and 5 Hz.

As can be seen in Figure 4.2b, LE has the highest cracking resistance among all specimens, followed by LA and LB. This superior cracking performance can be justified by the presence of lower RAP and higher binder content in their composition in comparison with the other studied mixtures. On the other hand, LD has the highest crack susceptibility based on the G-R_m parameter. An NCHRP 09-58 study recommended some values for the G-R_m parameter as a cracking performance indicator at intermediate temperatures. For instance, the maximum G-R_m value of 8000 MPa and 19000 MPa were recommended for the STA and LTA laboratory produced and compacted mixtures, respectively. Except for LD, other mixtures could pass the recommended threshold for STA mixtures. However, these threshold values may not be applicable for plant produced mixtures because they are subjected to reheating during the laboratory compaction procedure [20], [52]. Overall, the analysis of the parameters obtained from DM tests resulted in different performances for the studied mixtures.

4.1.2 Rutting Test Results

As the first step in evaluating rutting performance of the studied mixtures and identify a good surrogate test to assess NE mixtures, HWTT and IDEAL-RT tests were conducted, and the results are presented in Figure 4.3a and Figure 4.3b, respectively.

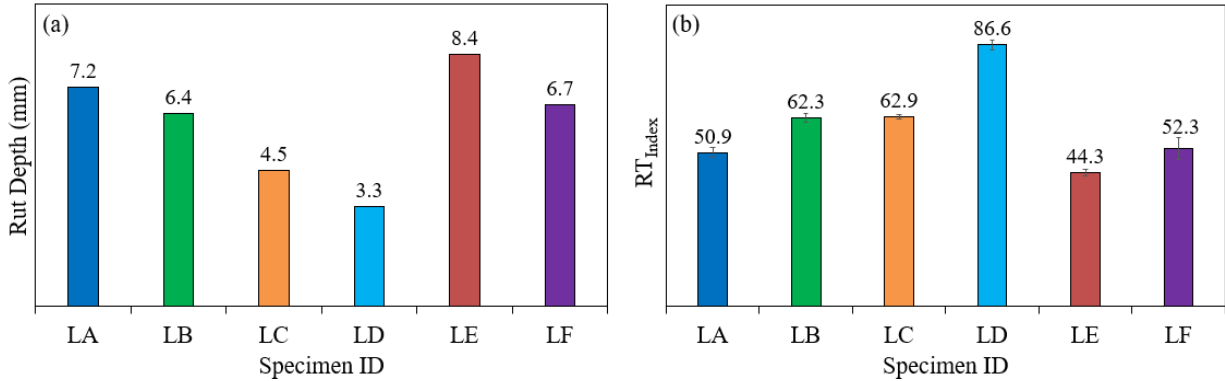


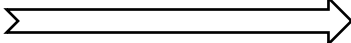
Figure 4.3 Rutting test results: (a) Rut depth (HWTT), and (b) RT_{Index} (IDEAL-RT).

For the HWTT test, the Illinois DOT criteria have been used based on the similarities in climate condition and binder grade utilization. With that, the total rut depth at 7,500 load cycles for PG 64-XX should be less than 12.5 mm [53]. Figure 4.3a indicates the total rut depth values at 7,500 load cycles. As seen, LD and LE had the lowest and highest rutting depth, respectively, which is a meaningful result considering the RAP content and binder content present in each mixture. LB and LA had total rutting depths of 6.39 mm and 7.24 mm, respectively. Compared to LB, LA contained ten percent more RAP and one percent more total binder content. This higher binder content seemed to contribute to a decreased rutting resistance in LA when compared to LB. Different specimens showed total rutting depth values of less than 12.5 mm, signifying they meet the rutting criteria. Overall, HWTT was capable of distinguishing mixture behavior effectively, which will be discussed in detail while comparing with the DM test results in the ensuing section.

Figure 4.3b shows the RT_{Index} results with a COV of 15% based on a limited dataset in this study, which shows the test is repeatable. As seen, similar to HWTT and $|E^*|$ results, LD and LE had the highest and lowest rutting resistance, respectively. However, with respect to statistical analysis, Tukey's honestly significant difference (HSD) test, LC and LB show no significant difference. The same situation applies to LF and LA, as the difference in results is not statistically significant (the analysis table is not included). The field data in the next section can further clarify the real difference between these specimens.

To explore the relationship between $|E^*|$ and different surrogate rutting tests, as well as surrogate tests to each other, a bivariate (Pearson) correlation analysis was performed to identify potential compatibility across various tests [54]. Table 4.1 shows the ranking of lab compacted specimens done by sorting the average mean value of each index from different test methods, while the cells with “,” represent the cases where the rankings are not statistically different among specimens. It should be noted that the IDT parameter and “G-stability/G-flow” parameter are adopted from Phase 1 of this study [4] to make this table more informative. With respect to Table 4.1, all the indices indicated LD and LE as the most and least resistant mixtures to rutting damages, respectively. Also, it is evident that for both HWTT and IDEAL-RT, a consistent rank order with $|E^*|$ is observed in terms of specimens' rutting performance. However, considering statistical analysis, some minor differences are captured; for instance, $|E^*|$ shows LA and LE are not statistically different, while RT_{Index} categorizes LF and LA as statistically similar specimens. In the case of HWTT, the rankings are solely based on rut depth values since no statistical analysis was available based on number of replicates. It is also observed that the order of ranking for HT-IDT and G-stability is slightly different from the other three tests, as LC and LA are switched in terms of rank orders.

Table 4.1 Ranking based on rutting resistance indices

Parameter	Least Resistant  Most Resistant					
$ E^* $	LA, LE	LA, LE	LF	LC, LB	LC, LB	LD
Rut depth	LE	LA	LF	LB	LC	LD
RT_{Index}	LE	LF, LA	LF, LA	LC, LB	LC, LB	LD
IDT	-	-	LC, LA	LC, LA	LB	LD
G-stability/G-Flow	-	-	LC, LA	LC, LA	LB	LD

Based on Figure 4.4, there was evidence of a correlation between $|E^*|$ vs. Rut depth and $|E^*|$ vs. RT_{Index} for the lab compacted specimens with a Pearson correlation value of 0.74 and 0.70, respectively (with 95% confidence level in all cases). With that, both the RT_{Index} and rut depth are highly correlated with the $|E^*|$ at 38 °C, 0.1 Hz. It should be noted that for $|E^*|$ vs. Rut depth there is an indirect relationship, while in the case of $|E^*|$ vs. RT_{Index} a direct relationship is governing. The relationship between $|E^*|$ vs. IDT and $|E^*|$ vs. G-stability was also analyzed with a moderate Pearson correlation of 0.4 and 0.44, respectively.

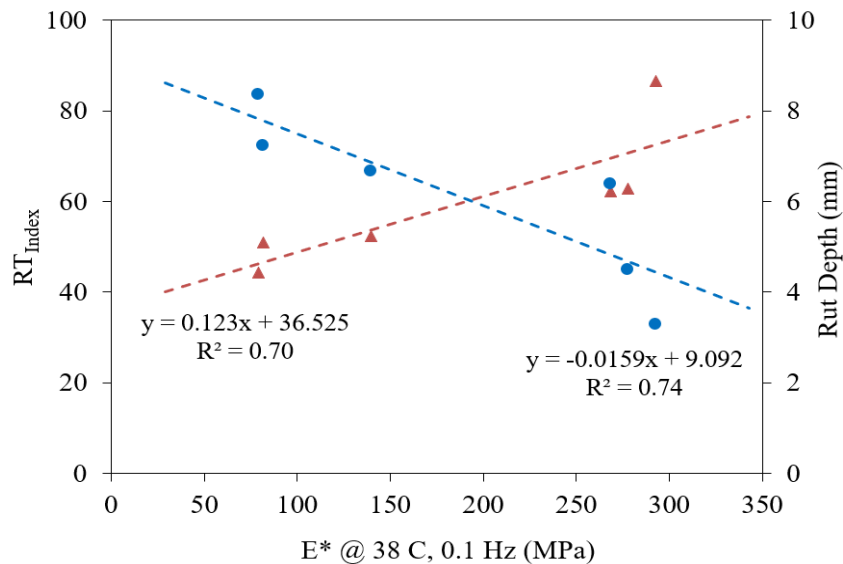


Figure 4.4 Correlation between DM vs. HWTT and DM vs. IDEAL-RT

Table 4.2 summarizes different factors evaluated in this study for the rutting indices from surrogate performance tests. Since four rutting tests were considered in this study, four different terms were defined to summarize the relative comparisons: Very High (VH), High (H), Moderate (M), and Low (L). Table 4.2 shows the relative comparison among tests considering the data provided in this study. For each parameter, the index that mostly satisfies the desired characteristics is shown in bold. As seen, RT_{Index} and Rut depth are two indices that met the highest satisfaction more than the two other parameters. As for HWTT, the variability analysis was not performed in this study, the common variability was reported to be within the range of 10 to 30% from literature [55]. With that, the RT_{Index} with a COV of less than 15% has an important advantage compared to rut depth parameter. With respect to the experience gained in this study, sample preparation, testing time, ease of use, and the cost of equipment for IDEAL-RT has an advantage over HWTT.

Table 4.2 Overall evaluation of rutting resistance indices

Parameter	Rut Depth	RT_{Index}	HT-IDT	G stability/G flow
Discrimination Potential	H	VH	M	M
Variability	H	M	M	M
Performance ranking	VH	H	M	M
Correlation with $ E^* $	H	H	M	M

Note: Very High (VH), High (H), Medium (M), Low (L) satisfaction

Overall, results indicate that asphalt mixtures incorporating higher RAP contents and lower binder contents typically demonstrate superior rutting resistance, as evidenced by multiple performance tests (DM, HWTT, and IDEAL-RT). These characteristics can be attributed to

increased stiffness modulus and reduced rutting susceptibility, making such mixtures particularly suitable for applications where rutting resistance is a primary concern. Conversely, mixtures with higher binder contents and lower RAP percentages generally exhibit reduced rutting resistance, potentially limiting their suitability in areas prone to rutting, such as regions with high temperatures or heavy traffic loads. Another important factor that needs to be considered to select a proper mix design is the aging level of RAP materials used. For instance, mixtures with similar design characteristics and same RAP content showed varying rutting resistance in this study, which emphasizes the importance of RAP aging characterization before any engineering applications.

4.1.3 Cracking Test Results

Figure 4.5 shows the FI results (average of three replicates) for the short- and long-term aged specimens. In terms of STA, LE and LA mixtures had the highest cracking resistance with FI values of 46.4 and 42.4, respectively. Accordingly, both LE and LA had the highest cracking resistance and rutting susceptibility based on the fundamental performance indicators, G-Rm and $|E^*|$, respectively. LD, LF, and LC (with 45% RAP—the highest RAP content among all) resulted in the most brittle and least crack resistant mixtures. Taking LB and LA into account, it is anticipated that LB would exhibit superior cracking resistance due to the lower RAP content in its mix design. However, in practice, LA displayed a higher FI value, which could be related to its higher asphalt content (6.3% for LA compared to 5.3% for LB) [56]. It appears that this higher asphalt content in LA counterbalanced the adverse impact of higher RAP content.

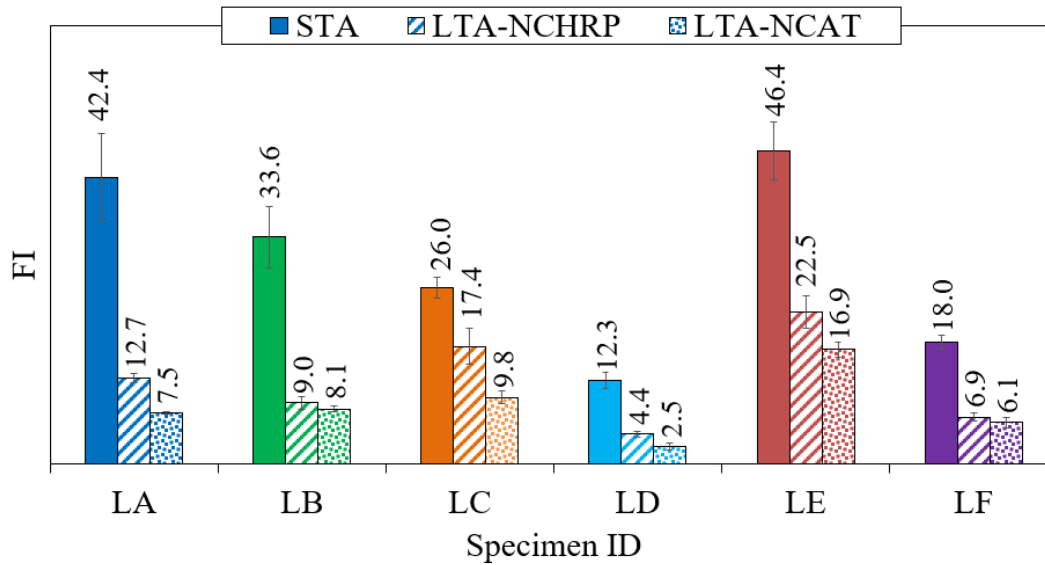


Figure 4.5 FI results for lab compacted specimens (STA and LTA)

The FI values of all specimens decreased following laboratory LTA; nonetheless, the rate of reduction varied across the featured mixture types and LTA protocols. For instance, with respect to the NCHRP protocol, LB with 25% RAP showed 73% reduction in the FI value, while for LC with 45% RAP this reduction was found to be 33%. This may be because RAP materials include binders that have already undergone some aging and do not age as aggressively under laboratory conditioning [57]. Compared to the NCHRP method, the NCAT protocol resulted in a higher rate of reduction in FI values for all types of specimens. This could signify a higher degree of aging induced by the NCAT protocol compared to the NCHRP protocol [58]. To further investigate and compare NHCRP and NCAT aging procedures, long-term field data, as well as binder level analyses are required. Considering the criteria set at an FI greater than 8.0 for the STA-conditioned specimens and exceeding 5.0 for the LTA ones [55], all specimens showed adequate resistance to cracking, except for the LD.

Another potential cracking resistance test considered for the sensitivity analysis of NE mixtures in this study was IDEAL-CT. Figure 4.6 indicates the average CT_{Index} values (based on three replicates) for the lab compacted specimens. In the case of STA, similar to FI and G-R_m parameters, LE and LD showed the highest and lowest crack resistance, respectively. However, in the case of LA and LB, the order was switched and did not align with I-FIT and DM test results. As expected, a significant drop was observed in the CT_{Index} values of all specimens subjected to LTA conditions. As a sensible observation, the highest drop in both LTA protocols (with the average of 79%) was observed in the LB specimen with the lowest amount of RAP in its mix design. Similar to FI, the CT_{Index} results also recorded a higher rate of reduction for NCAT compared to NCHRP protocol. In reviewing the literature, it was found that different U.S. state DOTs have their own pass/fail criteria for CT_{Index} values. For instance, the minimum values range from 32 in MoDOT to 100 at TxDOT for STA specimens [55].

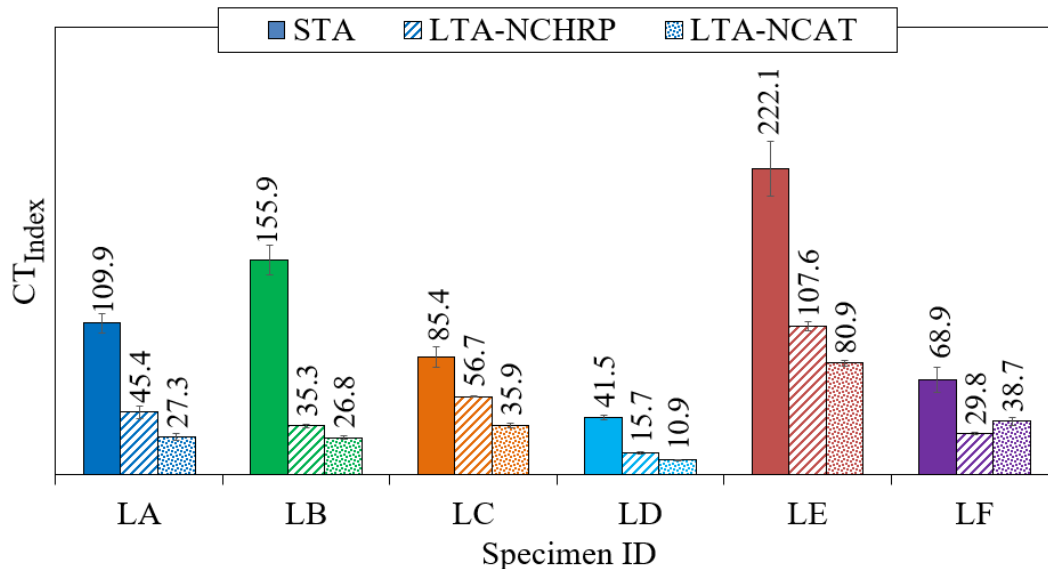


Figure 4.6 CT_{Index} results for lab compacted specimens (STA and LTA)

The I-bars in Figure 4.5 and Figure 4.6 represent the standard error of mean (SEM) derived from three replicates for each type of specimen. No data trimming (i.e., removing potential outlier) was applied on the results and the variability of each index was reported using the COV parameter. In the case of CT_{Index} , the COV ranged from 5.6% to 14.2% with an average of 10.2%. This range of COV was aligned with previous studies [26], [59]. The average COV for FI was observed to be 16% with a minimum and maximum COV of 6 and 18%, respectively. These COV values are based on the results from lab compacted specimens. With respect to the combined lab compacted and field core specimens, the COV values would be slightly higher for both tests. The higher variability of FI was reported in other studies and the reason might be associated with factors like stress concentration at the notch tip, crack propagation path, spatial distribution of aggregates along the crack tip, and accuracy of notching procedure on the resulting load-displacement curve [20], [59].

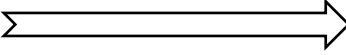
To assess the performance discrimination potential of various cracking indices, statistical analysis was conducted checking the normality assumption and equal variances at 95% confidence levels. The results showed the normal distribution and equal variance of all three indices. Accordingly, the one-way analysis of variance (ANOVA) at 95% confidence interval was carried out on three indices. The ANOVA results showed that the null hypothesis was rejected, and the Tukey's HSD test can be done. Table 4.3 shows the HSD test results for the cracking tests. For each parameter, the specimens that share the same letter are not statistically different in terms of average results. As seen, CT_{Index} and FI indicate five grouping letters, which show both tests have an acceptable sensitivity level, and can statistically discriminate the cracking performance of asphalt mixtures in this study.

Table 4.3 Tukey's HSD test results for cracking indices

Specimen ID	Cracking Index		
	FI	CT_{Index}	G-R _m
LA	ab	bc	c
LB	abc	b	b
LC	bcd	cd	b
LD	d	e	a
LE	a	a	d
LF	de	cd	b

The ranking of specimens based on different indices is presented in Table 4.4. This was performed by sorting the average value of each index from the most resistant to least resistant against cracking performance. As seen in Table 4.4, all three tests showed LE and LD as the most resistant and most susceptible specimens, respectively. The primary difference between the G-R_m parameter and the two parameters derived from surrogate tests (in STA condition), is related to LF and LC. However, this ranking difference was assumed to be irrelative, as the order of ranking was not statistically different considering the discrimination potential discussed earlier. Taking into account the two surrogate tests, FI and CT_{Index} are only different for the LA and LB specimens. Also, the significance of indices values is somewhat different in some cases among these two tests. The slight difference in ranking between these two tests can be attributed to the crack development and propagation mechanisms in strength-based and fracture-based tests, sample configurations in these tests, and mixture production variabilities, as reported by other researchers [60], [61]. However, when it comes to LTA specimens, a critical scenario for fatigue cracking in asphalt pavements, both performance tests consistently exhibit the same ranking order across all specimen types.

Table 4.4 Ranking based on cracking resistance indices

Index	Least Resistant 				Most Resistant	
G-R _m	LD	LC	LF	LB	LA	LE
FI	LD	LF	LC	LB	LA	LE
CT_{Index}	LD	LF	LC	LA	LB	LE
FI (LTA)	LD	LF	LB	LA	LC	LE
CT_{Index} (LTA)	LD	LF	LB	LA	LC	LE

Note: LTA = Long-term aged

To further investigate the relationship between cracking indices, a bivariate correlation analysis was performed to compare FI and CT_{Index} with each other and with the G-R_m parameter. Figure 4.7a indicates the relationships between G-R_m and other two indices, while Figure 4.7b represents the relationship between FI and CT_{Index} for the STA and LTA cases. Considering Figure 4.7a, both I-FIT and IDEAL-CT show a moderate to strong relationship with the G-R_m parameter, with R-squared values of 0.87 and 0.73, respectively. To have better insight into cracking performance of asphalt mixtures, it is essential to consider long-term aging. It is an established argument that long-term aging is a major factor controlling the fatigue cracking performance of asphalt mixtures [62]. That said, Figure 4.7b represents a strong direct relationship between CT_{Index} and FI after the long-term aging processing. With respect to these results, both IDEAL-CT and I-FIT can predict each other's cracking results in the case of long-term aged conditions. This observation can be attributed to the limited plasticity of brittle asphalt mixtures in both strength- and fracture-based tests [60]. It should be noted that the G-R_m parameter, as a linear viscoelastic property of materials, was suggested to indicate the potential for crack initiation in the early service life of asphalt pavements [20], [50]. As such, the need remains for comparing these surrogate cracking tests with a fundamental test such as BBF or cyclic fatigue test. Furthermore,

the field data, as well as mechanistical-empirical pavement design simulations are required to validate the outcomes and define the threshold values for the indices.

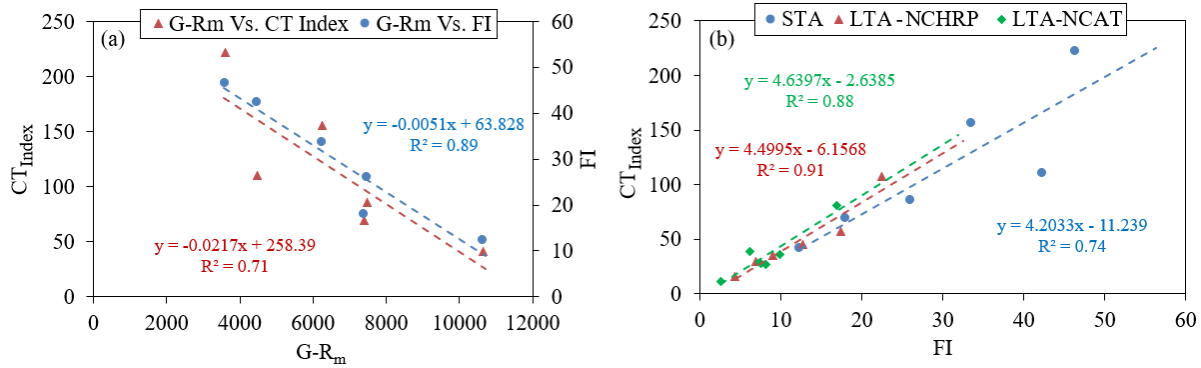
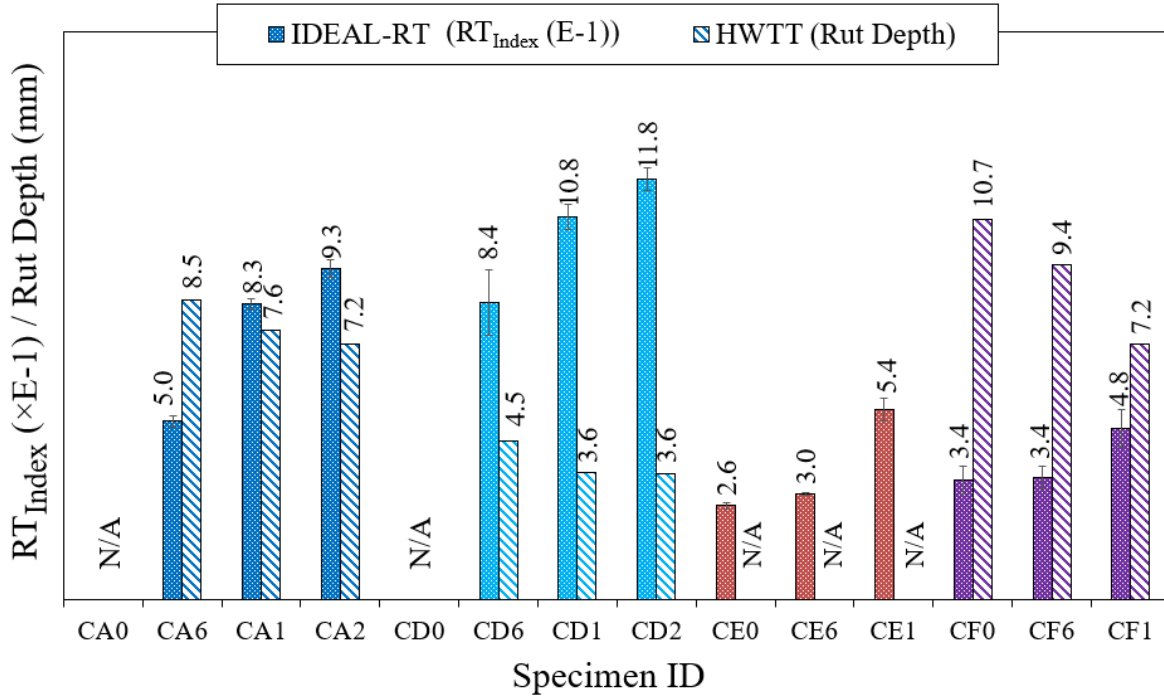


Figure 4.7 Correlation between (a) G-R_m vs. CT_{Index} , G-R_m vs. FI, and (b) FI vs. CT_{Index}

Considering mid-temperature cracking results, mixtures with lower RAP contents and higher binder contents generally demonstrated superior performance under both short- and long-term aging conditions, as indicated by FI and CT_{Index} parameters. This enhanced cracking resistance could be attributed to the improved flexibility provided by higher binder content and lower aged binder presence. Such mixtures are particularly suitable for applications where cracking is a primary concern, such as regions experiencing significant temperature fluctuations or heavy traffic loading. However, it should be noted, the decision on applicability of mixtures is highly dependent on many influential factors such as traffic conditions, environmental impacts, underlying layers and so on. Conversely, mixtures with higher RAP content demonstrated reduced cracking resistance across multiple test methods. This inverse relationship between rutting and cracking performance highlights the need for a BMD approach to ensure adequate performance across multiple distress types.

4.2 Step 2: Validation of Performance Tests Results Based on Field Assessment

To further validate step 1 findings, field data from the same projects were analyzed. This included performance test results from field core specimens and PMS data from surface measurements. The uniformity of pavement structural layers in various projects minimized the potential influence of underlying layers on HMA responses. For each type of distress, two performance tests selected from step 1 were used for the field core assessment. The field cores and PMS data were collected periodically during service life. Figure 4.8 shows the rutting depth and RT_{Index} results derived from HWTT and IDEAL-RT on the field core specimens, respectively. It should be noted that, for the field core specimens with lower thicknesses, the mix capping compound was used on the core bottoms to achieve the 62 ± 1 mm total core height for HWTT, while for the IDEAL-RT, thicknesses ranging from 38 to 95 mm are allowed. Four out of six projects are selected for this purpose (A, D, E, and F), and data collection is an ongoing task. As seen, for A and D projects, the field core specimens right after construction were not collected due to logistic issues. The first sensible observation is that as time passed, RT_{Index} and rut depth values increased and decreased, respectively, mainly due to the air void reduction and ongoing aging (stiffening) of the asphalt mixture over the pavement service life [63]. Furthermore, these changes in the results as the time passes signify the sensitivity of both rutting tests to the environmental conditions and ongoing stiffening of the pavements during service life. It is also noteworthy that the rank order of all four specimens based on field core performance test results shows the same trend as was observed in the lab compacted specimens in preceding sections.

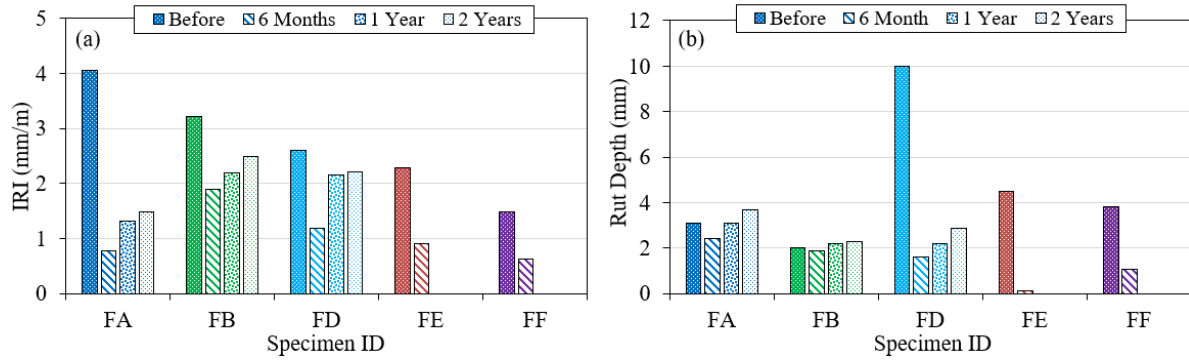


Note: CX = C stands for core samples; X stands for specimen ID; 0 = After Construction; 6 = 6 month after construction; 1 = 1 year after construction; 2 = 2 years after construction

Figure 4.8 IDEAL-RT and HWTT results of field core specimens during service life

The repeatability of IDEAL-RT was assessed in respect to COV, with a minimum and maximum COV of 3.5 and 12%, respectively, while the average COV for field core samples was observed to be 9%. With respect to reheating effects, compared to laboratory compacted specimens, the field cores could be considered as non-reheated specimens. In general, it is expected to see a superior rutting resistance for reheated specimens compared to non-reheated ones because of increased mixture stiffness due to reheating. The results show the significant effect of the reheating process, as rutting resistance is higher for lab compacted specimens compared to field core ones (higher RT_{Index} and lower rut depth values). However, it should be noted that the sample's variables for field cores are somewhat more than the lab compacted ones, i.e., air void or thickness of specimens.

The PMS data serve as an additional source for validating the results. Figure 4.9 presents the IRI, and rutting depth measurements obtained from road surfaces at the same reference points where field cores and loose mixtures were collected. While IRI and rutting are not directly related, IRI is a measure of road surface smoothness, which can be indirectly correlated with rutting performance. A pavement with high roughness (high IRI values) often experiences elevated stresses and strains under traffic loading, which can contribute to accelerated rutting. As seen in Figure 4.9a, FA, FB, and FD exhibited a gradual increase in IRI during the first two years of service life. In the case of FE and FF, the service life is still around one year, and the PMS data have yet to be received. Figure 4.9b shows the PMS data for rutting depth as a cumulative measure, since previous rut depths remain on the road surface. As such, the difference between consecutive reports is representative of rutting progress during that period. Accordingly, for instance, in the case of FA, after six months of service life, the reported rut depth was 2.4 mm. In the next time slot (one year), the rut depth value increased by 29%, reaching 3.1 mm. Subsequently, two years after construction, the rut depth increased by only 18%, attaining a value of 3.7 mm. This higher rutting resistance of the pavement over time agrees with performance test results from field core specimens and can be interpreted as validation of the performance test indices. Similar observations were also made in other cases.



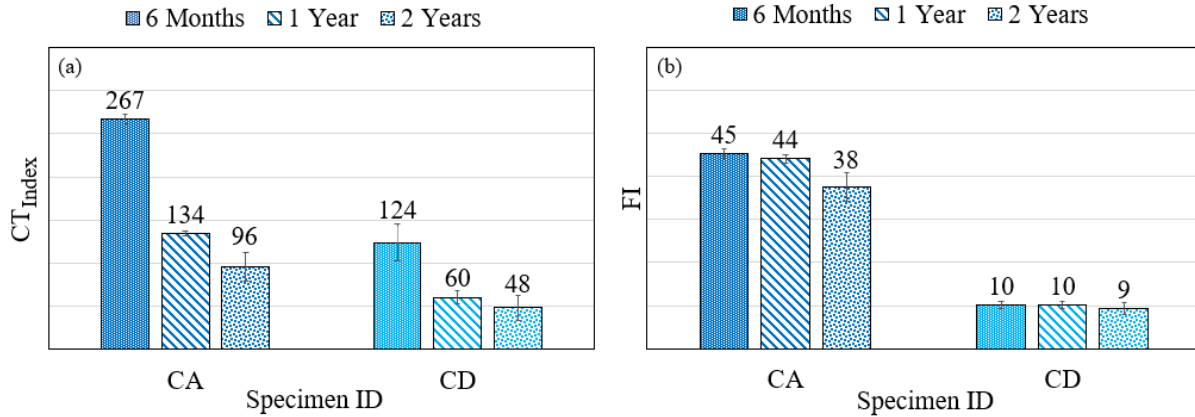
Note: FX = F stands for field data; X stands for specimen ID; IRI = International roughness index; Before = Before construction; 6 Months = 6 months after construction; 1 Year = 1 year after construction; 2 Years = 2 years after construction

Figure 4.9 The PMS data during service life (a) IRI, and (b) rut depth

The field core results for FI and CT_{Index} indices targeting CA and CD specimens are shown in Figure 4.10. The results are based on two years of field coring, however, specimens right after construction were not collected due to logistic issues. As seen, CT_{Index} decreased across the specimens, while in the case of I-FIT, the reduction of FI during this period is negligible. Generally, the longer exposure of a road to traffic load and environmental conditions is effective in coming up with higher cracking susceptibility, however, it is expected to observe the reduction in a long period of service life. With respect to PMS data, in the case of FA, zero amount of thermal and fatigue crack was recorded on the pavement surface during the first two years. In the case of FD, the fatigue crack values of 0.2, 0.32, and 0.35% were observed for six months, one year, and two years of service life, which are negligible. Comparing PMS data to cracking indices, the FI parameter seems to be more representative of reality in the field, as the field data during the first two years of service life are not that different. It is important to mention that IDEAL-CT, as a strength-based test, accounts for energy dissipation due to both plastic deformation and cracking evolution, while in the I-FIT, plastic deformation effects are more limited. With that, it is expected to see more diverse results from these two tests when comparing field projects where high tensile

strains are developed in sooner stages, such as in thin pavements or at the beginning of service life, as explained in other studies [60], [61]. However, as mentioned in the preceding section, for the cracking resistance, long-term performances are governing, in which, both FI and CT_{Index} showed comparable results after long-term aging conditioning.

An average COV of 13.4 and 12% was recorded for CT_{Index} and FI of field core specimens, respectively. This indicates similar and acceptable levels of repeatability for these two tests, based on the limited dataset in this study. Another important consideration is the reheating effect on the index's values. It was expected to see higher cracking resistance (higher CT_{Index} and FI) for field core specimens as they have not undergone the reheating process. This was observed for CT_{Index} , where the values for field cores were significantly higher than those of lab compacted specimens. In the case of FI, the difference between these two sets of specimens was insignificant. However, there is a lack of literature and experience in evaluating the CT_{Index} for field cores, which typically have a reduced thickness. As a result, further assessment is needed to validate the effectiveness of the correction factor used to relate field cores to lab-compacted specimens. Overall, to better leverage field data for evaluating cracking performance, the collection of long-term data is required.



Note: 6 Months = 6 months after construction; 1 Year = 1 year after construction; 2 Years = 2 years after construction; CX = C stands for core samples; X stands for specimen ID; Values inside the columns = Average air void of 3 core specimens

Figure 4.10 IDEAL-CT and I-FIT results of field core specimens during service life

4.3 Summary of the Tests' Key Characteristics

With respect to the experimental and statistical findings from evaluation of various monotonic performance-based tests for potential implementation in a BMD framework, Table 4.5 presents a summary of properties associated with each test's key characteristics. According to Table 4.5, IDEAL-RT, HT-IDT, G-stability, and IDEAL-CT demonstrate superior cost-effectiveness in terms of equipment expenses and time allocation, including sample preparation, conditioning, and testing procedures. The complexity of data analysis is classified in two groups: those requiring simple analysis and those demanding fair complexity; in which, only HWTT is listed as fair, while the remaining performance tests show relatively simple analytical requirements. The variability analysis indicates an acceptable range of COV for most performance tests, though I-FIT and HWTT have higher COV values compared to other tests, based on the results from this study and existing literature. Taking these parameters into account, the tests' practical applicability for potential mixture design and quality control phases within a BMD

framework for highly recycled polymer modified asphalt mixtures has been categorized as either Good or Fair, with the results demonstrated in Table 4.5.

Table 4.5 Summary of practical applicability of different performance-based tests

Test Method	Cost Approximate	Testing Time (hour)	Data Analysis Complexity	Test Variability (%)	Field Validation	Practicality
HWT (AASHTO T 324)	\$\$\$\$ (Including saw machine)	8-9 (Including cutting and conditioning)	Fair	10-30	More Data Required	Good for Mix Design Fair for QA
HT-IDT (ALDOT-458)	\$ (Including conditioning)	3 (Including conditioning)	Simple	~15		Good for Mix Design Good for QA
IDEAL-RT (ASTM under preparation)	\$ (Including conditioning)	3 (Including conditioning)	Simple	15		Good for Mix Design Good for QA
G-stability (Nsengiyumva et al., 2020)	\$ (Including conditioning)	3 (Including conditioning)	Simple	~15		Good for Mix Design Good for QA
I-FIT (AASHTO - T 393)	\$\$ (Including cut and saw machine, conditioning)	4 (Including cutting and conditioning)	Simple	~16		Good for Mix Design Fair for QA
IDEAL-CT (ASTM D 8225)	\$ (Including conditioning)	3 (Including conditioning)	Simple	~10		Good for Mix Design Good for QA

Chapter 5 Preliminary Threshold Criteria for Performance Tests

After selecting appropriate performance tests for potential implementation in the BMD framework, the next step was to establish initial pass/fail criteria for each test based on the data provided in this study. To this goal, experimental results and field data were adopted in combination with a mechanistic empirical pavement design guide (MEPDGG) methodology. The use of MEPDGG results was adopted to predict long-term field performance to support our recommended initial threshold criteria, since only short period (<3 years) field data are available at this stage. The MEPDGG approach involved predicting the service life of various pavement projects, accounting for structural layers, climate conditions, traffic volumes, and other project-specific information. These predicted service lives were compared to the field data from PMS data collection to validate the design assumptions and initial predictions. Afterward, representative pavement structural layers in Nebraska were adopted, and mechanistic-empirical design was conducted using various AC layers. The performance test indices associated with each AC layer were then compared to its predicted service life to determine the value of each index that would meet the required pavement service life. These values of indices were established as preliminary threshold values for each performance test.

5.1 Introduction to the MEPDG Method

The MEPDG is an improved methodology for pavement design and the evaluation of paving materials analyzing both new and rehabilitated pavement structures using mechanistic-empirical principles. Unlike currently used empirical-based pavement design methods, this methodology depends heavily on the characterization of the fundamental engineering properties of paving materials. This approach calculates pavement responses (including stresses, strains, and deflections) and uses these measurements to determine incremental damage accumulation over

time [64]. The system then connects this cumulative damage to observable pavement deterioration through empirical relationships. This process is visually represented in Figure 5.1. The commercial implementation of this methodology is available as AASHTOWare Pavement ME Design® software. The AASHTOWare represents a fundamental shift in pavement design methodology. It forecasts multiple performance indicators (shown in Figure 5.1) while establishing direct connections between materials, structural design, construction methods, climate conditions, traffic patterns, and pavement management systems [64].

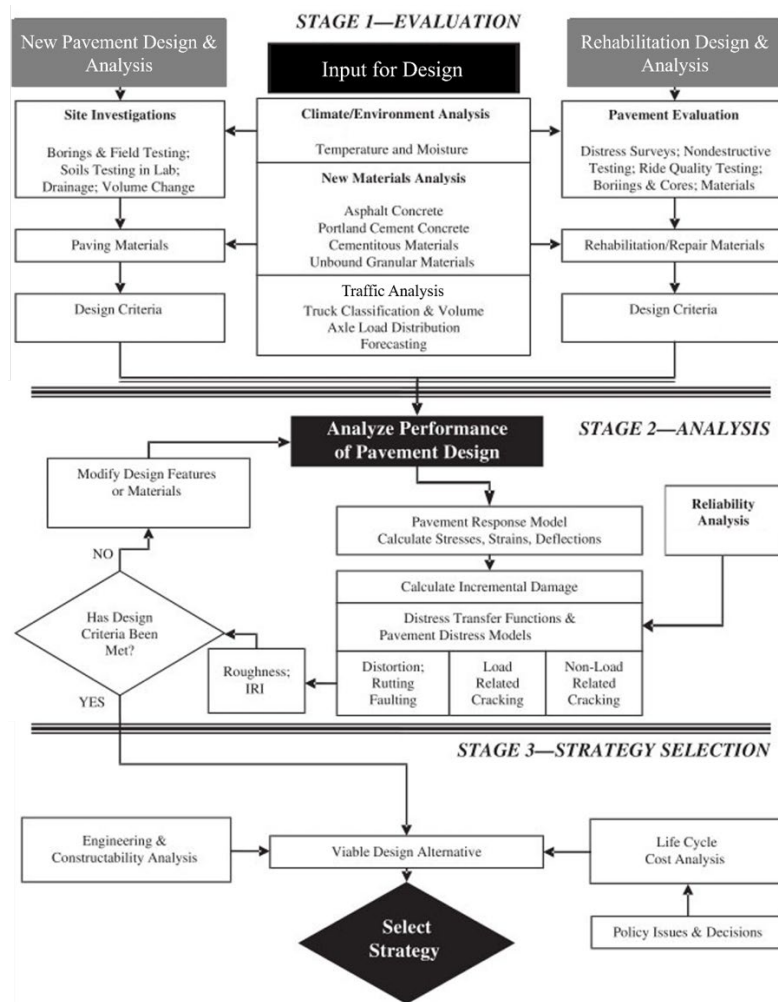


Figure 5.1 Conceptual Flowchart of the Three-Stage Design/Analysis Process for AASHTOWare (Adopted from [64])

The MEPDG approach combines engineering mechanics with real-world observations to create a rational design process. This framework consists of three key elements: 1) The mechanistic part which is prediction of pavement responses (strains, stresses, deflections) based on traffic and climate conditions; 2) materials characterization which is aligned with the theoretical approach; and 3) establishing relationships between these responses and actual observed pavement distress (the empirical part). The MEPDG offers comprehensive procedures for analyzing both new and rehabilitated flexible and rigid pavements using consistent parameters across all pavement types.

The AASHTOWare outputs are primarily the predicted distresses and IRI at specified reliability levels throughout a pavement design life. Its thickness optimization capabilities enable both analysis and design functions by evaluating various combinations of materials, layer thicknesses, and design features against specific site conditions and failure criteria. This evaluation occurs at a predetermined reliability level over a specified time period, allowing engineers to develop optimal pavement designs for diverse conditions and requirements [64].

The MEPDG employs a hierarchical input scheme with three distinct levels to categorize the designer's knowledge of input parameters for material and traffic data. Input Level 1 represents the highest level of knowledge, using directly measured, site-specific data, though it incurs the highest testing and collection costs; this level is particularly valuable for projects with unusual features outside the standard inference space. Level 2 parameters are estimated from correlations or regression equations using less costly site-specific measurements, or they may represent regional values that aren't project-specific. Level 3 relies on "best-estimated" or default values based on global or regional medians from similar datasets, offering the lowest knowledge precision but also the lowest data collection costs.

5.1.1 Distress Prediction Equations for Flexible and Semi-Rigid Pavements

In the MEPDG methodology, pavement trial designs are broken down into sublayers, with thicknesses determined by material type, actual layer dimensions, and depth position within the overall structure. For calculating critical pavement responses within each sublayer, the system employs JULEA, an elastic layer theory program embedded in the AASHTOWare software. Additionally, the MEPDG extensively utilizes the Enhanced Integrated Climatic Model (EICM) to adjust pavement layer modulus values based on temperature and moisture conditions, which are calculated on an hourly basis throughout the entire pavement structure.

The MEPDG uses dynamic modulus to calculate critical strains for determining maximum permanent deformation and fatigue damage in HMA layers. The ICM provides hourly temperature calculations that enable estimation of HMA properties for transverse crack prediction and adjusts the resilient modulus of unbound layers based on freezing-thawing cycles and monthly moisture content variations relative to optimum levels. These calculated pavement responses serve as inputs to mathematical models that predict fatigue damage, thermal cracking, and permanent deformation, forming the foundation of performance indicator predictions throughout the analysis period.

5.1.2 Rutting Depth

The MEPDG approach to rutting prediction calculates incremental permanent deformation at the mid-depth of each sublayer within the pavement structure. This method sums the plastic vertical deformations across all layers to determine total rutting for each analysis period. The model incorporates a "strain hardening" approach that accounts for varying conditions from month to month while accumulating plastic vertical strains in a cumulative deformation framework. For material characterization, repeated load permanent deformation triaxial tests are conducted on both

HMA mixtures and unbound materials to determine their deformation behavior under cyclic loading. These laboratory-derived relationships are subsequently calibrated using field measurements to ensure the predicted rutting matches actual pavement performance, with the field-calibrated form for HMA mixtures expressed in Equation 5.1:

$$\Delta_{p(HMA)} = \epsilon_{p(HMA)} h_{(HMA)} = \beta_{1r} k_z \epsilon_{r(HMA)} 10^{k_1} n^{k_2 \beta_2} T^{k_3 \beta_3} \quad (5.1)$$

Where $\Delta_{p(HMA)}$ =Accumulated permanent or plastic vertical deformation in the HMA layer/sublayer (in.), $\epsilon_{p(HMA)}$ =Accumulated permanent or plastic axial strain in the HMA layer/sublayer (in/in.), $\epsilon_{r(HMA)}$ =Resilient or elastic strain calculated by the structural response model at the mid-depth of each HMA sublayer (in/in.), $h_{(HMA)}$ =Thickness of the HMA layer/sublayer (in.), n =Number of axle-load repetitions., T =Mix or pavement temperature (°F), k_z = Depth confinement factor, $k_{1,2,3}$ = Global field calibration parameters, and $\beta_{1,2,3}$ = Local or mixture field calibration constants; for the global calibration, these constants were all set to 1.0.

The field-calibrated mathematical equation used to calculate plastic vertical deformation within all unbound pavement sublayers and the foundation soil could be found elsewhere [64].

5.1.3 Load-Related Cracking

The MEPDG predicts two load-related cracking types in flexible pavements: alligator cracking, which initiates at the HMA bottom and propagates upward, and longitudinal cracking, which begins at the surface. Both utilize the same incremental damage approach with critical axle-load applications calculated by Equation 5.2a, though with different critical locations and calibration parameters to reflect their distinct failure mechanisms.

$$N_{f-HMA} = K_{f1}(C)(C_H)\beta_{f1}(\epsilon_t)^{k_{f2}\beta_{f2}}(E_{HMA})^{k_{f3}\beta_{f3}} \quad (5.2a)$$

Where N_{f-HMA} = Allowable number of axle-load applications for a flexible pavement and HMA overlays, ϵ_t = Tensile strain at critical locations and calculated by the structural response model (in./in.), E_{HMA} = Dynamic modulus of the HMA measured in compression (psi), $k_{f1,f2,f3}$ = Global field calibration parameters, and $\beta_{f1,f2,f3}$ = Local or mixture specific field calibration constants; for the global calibration effort, these constants were set to 1.0.

$$C = 10^M \quad (5.2b)$$

$$M = 4.84 \left(\frac{V_{be}}{V_a + V_{be}} - 0.69 \right) \quad (5.2c)$$

Where: V_{be} = Effective asphalt content by volume (%), V_a = Percent air voids in the HMA mixture, and C_H = Thickness correction term, dependent on type of cracking. For bottom-up or alligator cracking:

$$C_H = \frac{1}{0.000398 + \frac{0.003602}{1 + e^{(11.02 - 3.49H_{HMA})}}} \quad (5.2d)$$

For top-down or longitudinal cracking:

$$C_H = \frac{1}{0.01 + \frac{12.00}{1 + e^{(15.676 - 2.8186H_{HMA})}}} \quad (5.2e)$$

Where H_{HMA} = Total HMA thickness (in.).

The area of alligator cracking and length of longitudinal cracking are calculated from the total damage over time using different transfer functions, with the detailed equations provided elsewhere [64].

In semi-rigid pavements, for calculating fatigue cracks in rigid layers, the allowable number of load applications, N_{f-CTB} , is determined in accordance with Equation 5.3a and the amount or area of fatigue cracking is calculated in accordance with Equation 5.3b:

$$N_{f-CTB} = 10^{\left[\frac{k_{c1}\beta_{c1}\left(\frac{\sigma_1}{M_R}\right)}{k_{c2}\beta_{c2}} \right]} \quad (5.3a)$$

$$FC_{CTB} = C_1 + \frac{C_2}{1 + e^{(C_3 - C_4 \log(DI_{CTB}))}} \quad (5.3b)$$

Where N_{f-CTB} = Allowable number of axle-load applications for a semi-rigid pavement, M_R = 28-day modulus of rupture for the CTB layer (psi), DI_{CTB} = Cumulative damage index of the CTB or cementitious layer, $k_{c1,c2}$ = Global calibration factors, $\beta_{c1,c2}$ = Local calibration constants, FC_{CTB} = Area of fatigue cracking (sq ft), and $C_{1,2,3,4}$ = Transfer function regression constants.

5.1.4 Non-Load-Related Cracking-Transverse Cracking

The thermal cracking model in the MEPDG is an enhanced version of work developed under the Strategic Highway Research Program (SHRP) A-005 research contract [65]. This model predicts crack propagation resulting from thermal cooling cycles using the Paris law of crack propagation, which relates the rate of crack growth to the range of stress intensity factors experienced during temperature fluctuations, as shown in Equation 5.4:

$$\Delta C = A (\Delta K)^n \quad (5.4)$$

Where: ΔC = Change in the crack depth due to a cooling cycle, ΔK = Change in the stress intensity factor due to a cooling cycle, and A, n = Fracture parameters for the HMA mixture.

Experimental results indicate that reasonable estimates of A and n can be obtained from the indirect tensile creep-compliance and strength of the HMA, using equations detailed elsewhere [64].

The degree of cracking is predicted by the MEPDG using an assumed relationship between the probability distribution of the log of the crack depth to HMA-layer thickness ratio and the percent of cracking. Equation 5.5 shows the expression used to determine the extent of thermal cracking:

$$TC = \beta_{t1} N \left[\frac{1}{\sigma_d} \text{Log} \left(\frac{C_d}{H_{HMA}} \right) \right] \quad (5.5)$$

Where: TC=Observed amount of thermal cracking (ft/mi), β_{t1} = Regression coefficient determined through global calibration, N= Standard normal distribution, σ_d = Standard deviation of the log of the depth of cracks in the pavement (in.), C_d = Crack depth (in.), and H_{HMA} = Thickness of HMA layers (in.).

5.1.5 Reflective Cracking in HMA Overlays

Paris-Erdogan's law is used to model reflective crack propagation from rigid layers to the HMA overlays. The transfer function is used to estimate the amount of fatigue and transverse cracks exhibited in a non-surface layer that reflect to the AC surface or overlay after a certain period of time. This transfer function predicts the percentage of area of cracks that propagate through the AC as a function of time, as shown in Equation 5.6 due to wheel loads, and in Equation 5.7 for temperature changes:

$$\frac{dc}{dN} = A(\Delta k)^n \quad (5.6)$$

$$\frac{dc}{dT} = A(\Delta k)^n \quad (5.7)$$

Where c = Crack length and dc is the change or growth in crack length, N = Number of loading cycles and dN is the increase in loading cycles during a time increment, T = Temperature and dT is the increase in thermal cycles during a time increment, ΔK = Stress intensity amplitude that

depends on the stress level, the geometry of the pavement structure, the fracture model, crack length, and load transfer efficiency across the crack or joint, A , n = Fracture parameters specific to the asphalt concrete mixture.

The fracture properties A and n are calculated from the indirect tensile creep-compliance and strength of the AC mixture in accordance with Equations 5.8a and 5.8b:

$$A = g_2 + \frac{g_3}{m_{mix}} (\log D_1) + g_4 \log \sigma_t \quad (5.8a)$$

$$n = g_0 + \frac{g_1}{m_{mix}} \quad (5.8b)$$

Where $g_{0,1,2,3,4}$ = Mixture regression coefficients, m_{mix} = The log-log slope of the mixture creep compliance versus loading time relationship for the current temperature and loading time, D_1 = Coefficient of creep compliance expressed in the power law form, σ_t = Tensile strength of the AC mix at the specific temperature.

The three response mechanisms are used to estimate the change in crack length over time: bending, shear, and tension. The crack growth or damage increment from each mechanism is provided in Equation 5.9:

$$\Delta_{Bend} = A(\Delta k_B)^n \quad (5.9a)$$

$$\Delta_{Shear} = A(\Delta k_S)^n \quad (5.9b)$$

$$\Delta_{Tension} = A(\Delta k_T)^n \quad (5.9c)$$

The loading time for the bending and shear mechanisms (Equations 5-9a and 5-9b) are defined in a similar way to the loading time for the alligator fatigue cracking model, while the loading time for the tensile mechanism (Equation 5-9c) is defined in a similar way to the low temperature cracking model. The stress intensity factors (ΔK) for each mechanism are determined

using neural networks, which are similar in concept to those developed for the rigid pavement distress prediction models. The reflection cracking neural network models were developed from finite element analyses for the MEPDG family of pavements, as detailed elsewhere [64].

5.2 Design Inputs and Structural Layer Properties Considered in this Project

Among the six different projects used in this study, four were selected for criteria determination. Project B and C were eliminated from this phase of the study, as project B was implemented on a bridge, and in project C, the asphalt mixture was collected from the second layer of the pavement, not the top-lift layer. Consequently, projects A, D, E, and F were adopted for criteria selection.

The performance criteria for the MEPDG method were selected based on the requirements of the Nebraska state as specified in the NDOT pavement design manual [66], and the average accepted values in different states, with a comprehensive list presented in Table 5.1. For design reliability, a value of 90% was selected for all the projects [66].

Table 5.1 Rating scale for pavement condition [66]

Rating	Good	Fair	Poor
IRI (mm/m)	<1.50	1.50 – 2.68	>2.68
Cracking Percent (%)	<5	5-20	>20
Rutting (mm)	<4	4-9	>9

The traffic data associated with each project design, including average annual daily truck traffic (AADTT), were obtained from Nebraska DOT resources (Figure 5.2), while the detailed information about vehicle types, axle distribution, and other parameters was adopted from the default values in AASHTOWare. The default normalized axle-load spectra for each axle type and

normalized truck classification volume distribution for the 17 different truck traffic classification (TTC) groups included in the AASHTOWare were determined from analyzing the traffic data collected on over 180 long-term pavement performance (LTPP) test sections.

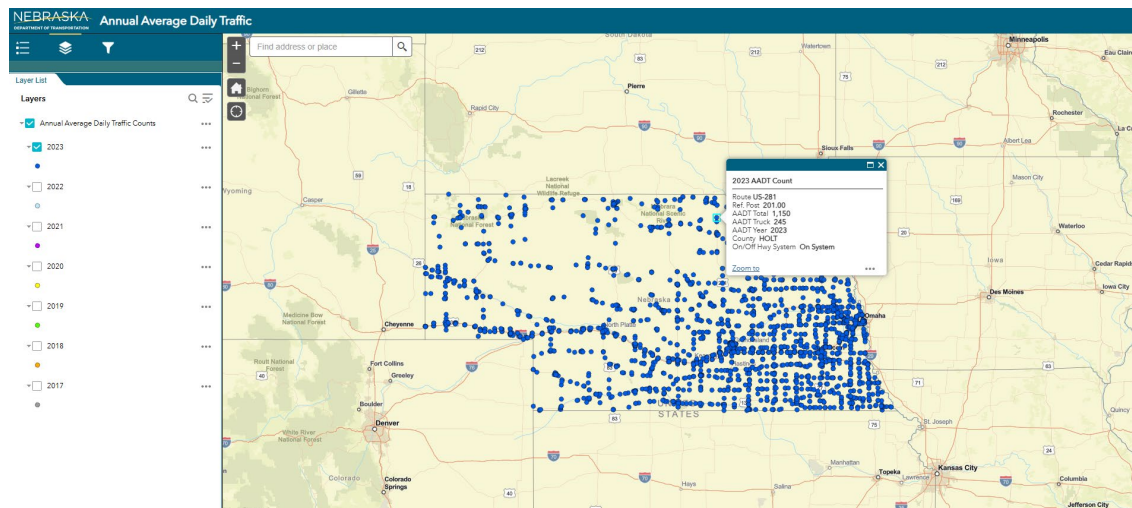


Figure 5.2 Traffic data (AADTT) adoption for each project

The climate data associated with each project location was acquired from MERRA-2 climate dataset, provided by FHWA. The structural layers representative of each project is shown in Figure 5.3. As can be seen, except for LA, the other three projects have Portland cement concrete (PCC) as a structural layer underneath the pavement. For the AC layer inputs, the mechanical and rheological properties were incorporated as level 1, since the dynamic modulus was measured at different temperatures and frequencies (Figure 4.1), and the DSR test was conducted to measure rheological properties at three different temperatures (Table 5.2). For the underlying structural layers, the mechanical properties were added based on level 3 hierarchical inputs. Figure 5.4 presents soil types associated with the subgrade layer of each project along with the resilient modules corresponding to each soil type [67]. In all the design efforts, overlay/rehabilitation was

selected for the design type, since all the projects involved milling an old pavement and rehabilitation with a new AC layer.

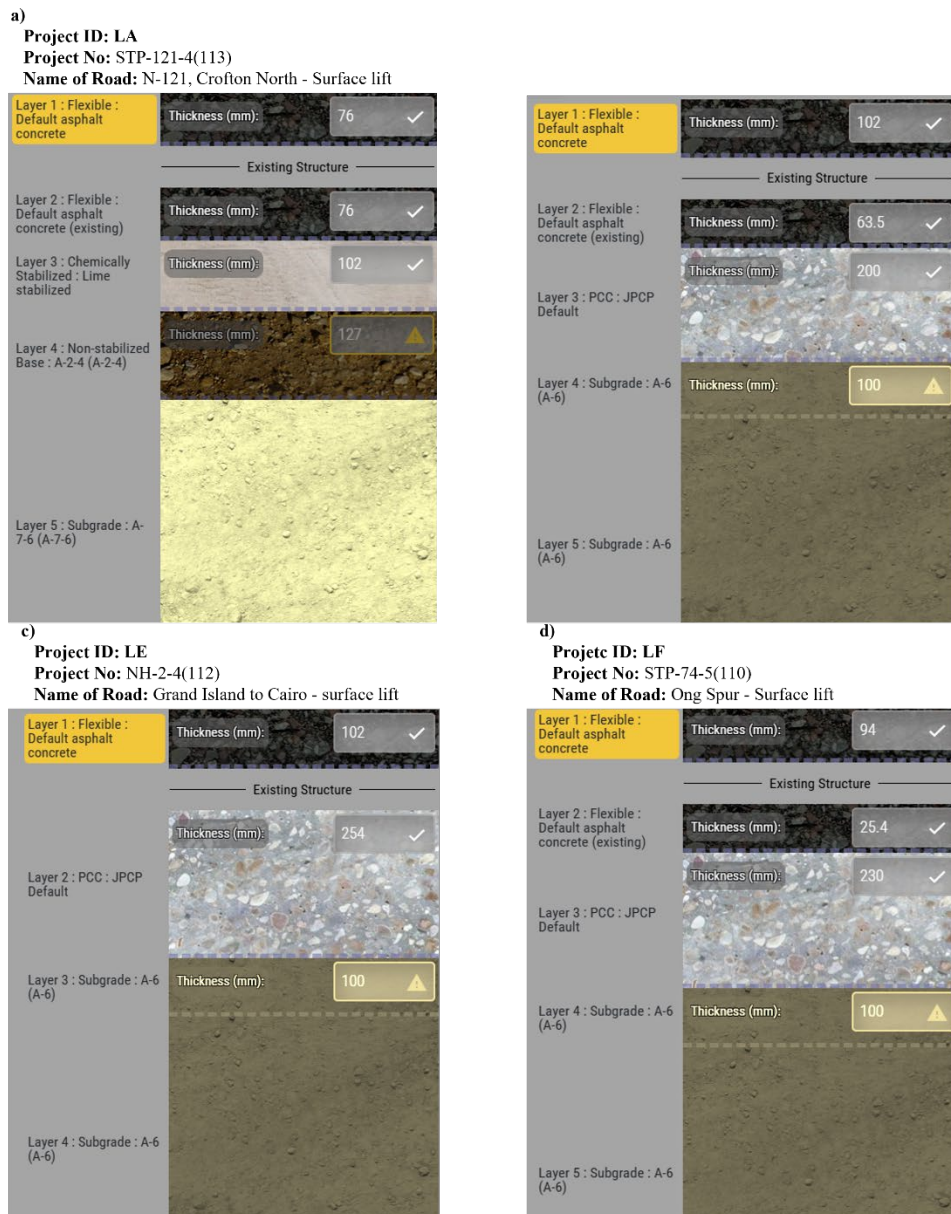


Figure 5.3 Projects' structural layers for mechanistic-empirical pavement design

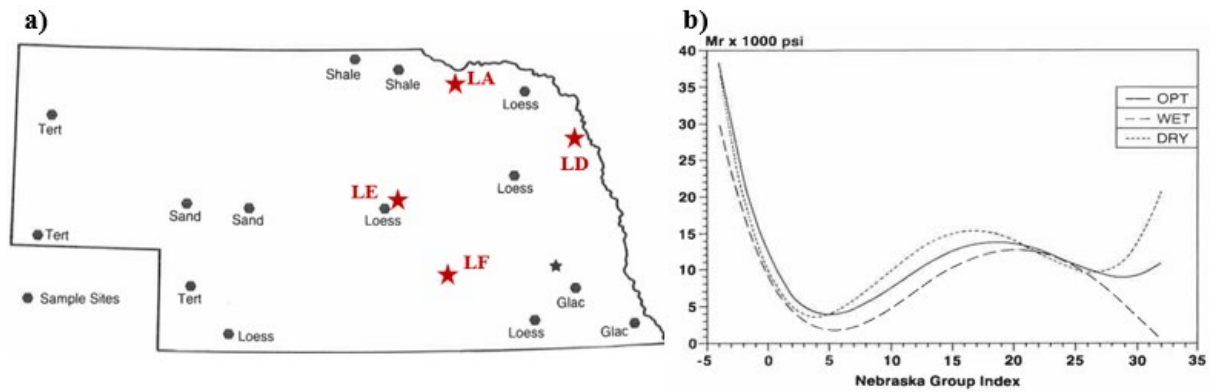


Figure 5.4 a) soil types in Nebraska and project locations, and b) resilient modulus vs. Nebraska group index of soils [67]

The information associated with each road section—number of lanes in each direction, road condition before milling and rehabilitation, thickness of milling, etc.—was adopted considering the information provided by NDOT TAC members. Google map images were further assessed to confirm the number of lanes in each section (Figure 5.5).

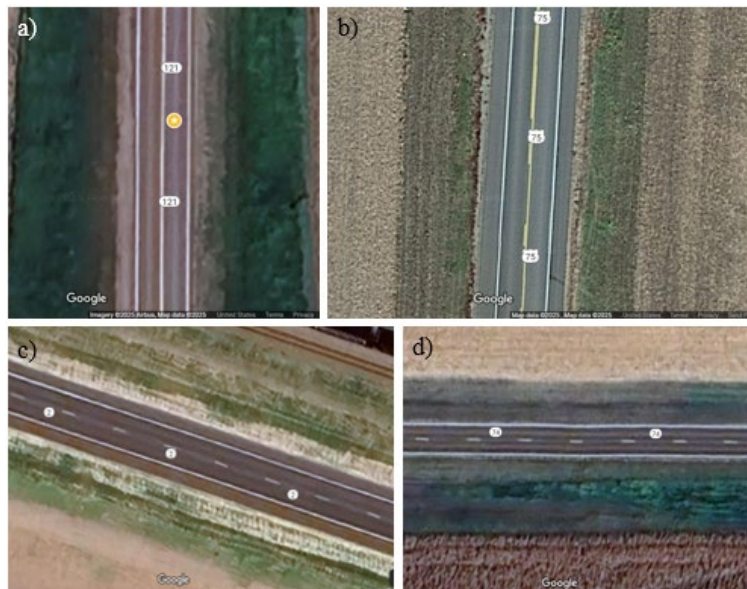


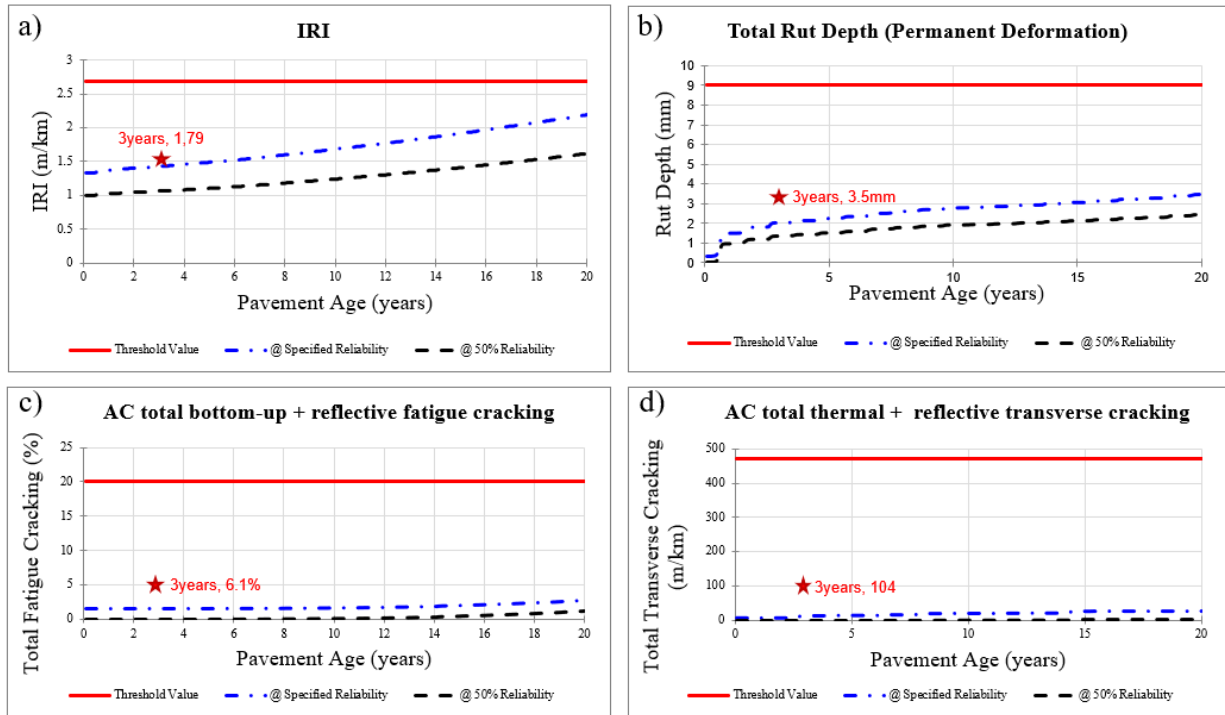
Figure 5.5 Road section and lane numbers (pictures adopted from Google map): a) LA, N-121, Crofton North, b) LD, US-75, Tekamah, c) LE, Highway 2, Grand Island to Cairo, d) LF, US-74, Ong spur

Table 5.2 Rheological properties of asphalt binders in each project using DSR test

Mix ID	58 °C		64 °C		70 °C	
	δ (degree)	G^* (kPa)	δ (degree)	G^* (kPa)	δ (degree)	G^* (kPa)
LA	70.53	11.93	72.02	5.81	73.78	2.95
LD	72.80	9.97	74.71	4.72	76.75	2.32
LE	66.10	10.58	67.51	5.12	69.01	2.84
LF	68.76	13.16	70.67	6.35	72.82	3.18

5.3 Validation of MEPDG Assumptions using Field Data

Using the parameters mentioned in the previous section, the MEPDG design was conducted for each project to predict the service life based on pavement structural layer data. The design results for each project are presented in Figure 5.6 to Figure 5.9. As shown, four main parameters were selected as outputs for each project design: IRI, total rut depth, AC bottom-up + reflective fatigue cracking, and AC total thermal + reflective transverse cracking. For each project, the field data collected by the pavement management system during the past two to three years of service life are also indicated with red star on each graph.

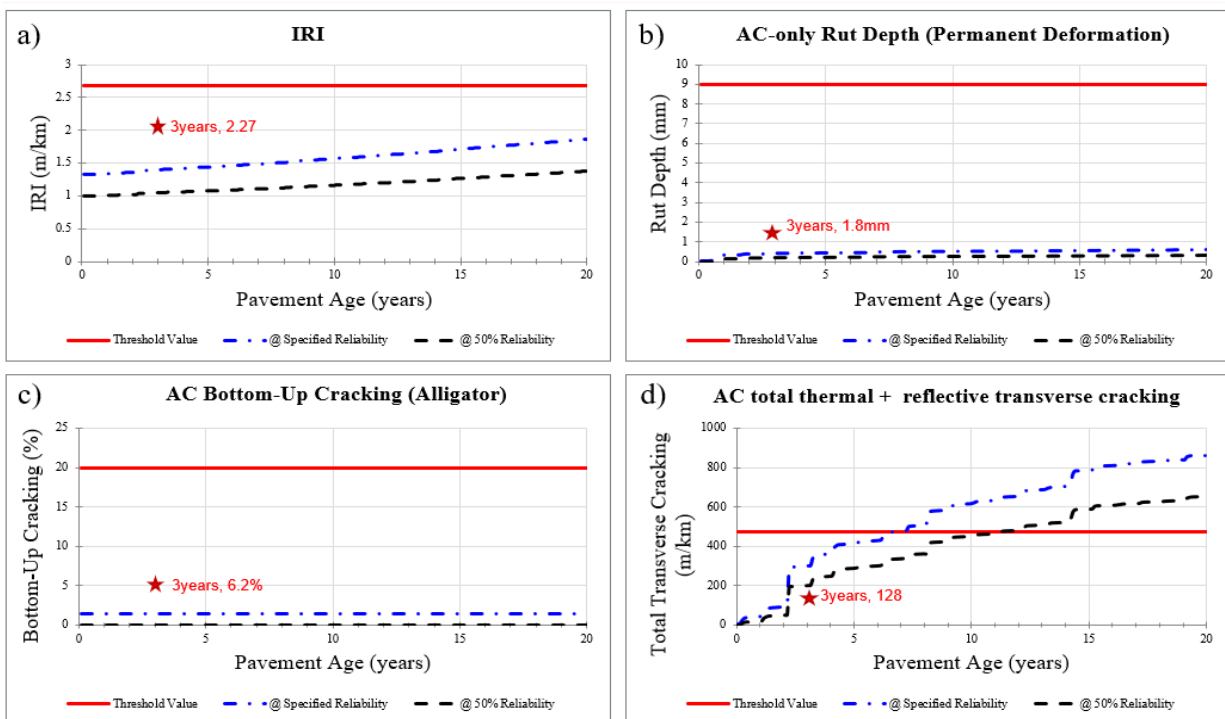


Note: Red star (*) is used to show PMS data

Figure 5.6 Mechanistic-empirical pavement design and PMS data for LA project (Crofton)

Based on Figure 5.6, in the case of LA, the only pavement with no PCC structure underneath, none of the parameters will reach the threshold value before 20 years of service life. Among different parameters, IRI and rut depth appear to be the critical ones that could potentially control the design, while both cracking parameters indicate no concern regarding pavement cracking. Figure 5.7 indicates the MEPDG for the LD project along with PMS data collected during service life. As noted in Figure 5.3, LD has a PCC layer underneath the pavement surface, which makes reflective transverse cracking the dominant type of crack based on MEPDG methodology. Reflective cracks can be caused by horizontal movements from the expansion and contraction of the PCC slabs that are concentrated at the joints and cracks, and from increased vertical deflections at these locations. These horizontal movements result from temperature changes in the PCC slab. The development of reflective cracking due to environmental loading

dependent on the magnitude and rate of temperature change, slab geometry, gauge length across the joint or crack, and properties of the resurfacing material or overlay. Due to the bond between the HMA overlay and existing pavement, the tensile stresses and strains produced from joint movements become critical in the areas of the PCC joints and cracks [68]. Based on the results, rutting is not a concern for this pavement structure, however, reflective transverse cracking is limiting the pavement's service life. It should be noted that the results in Figure 5.6 and Figure 5.7 reflect the overall performance of different pavement structural layers, not only the top-lift (surface) layer.

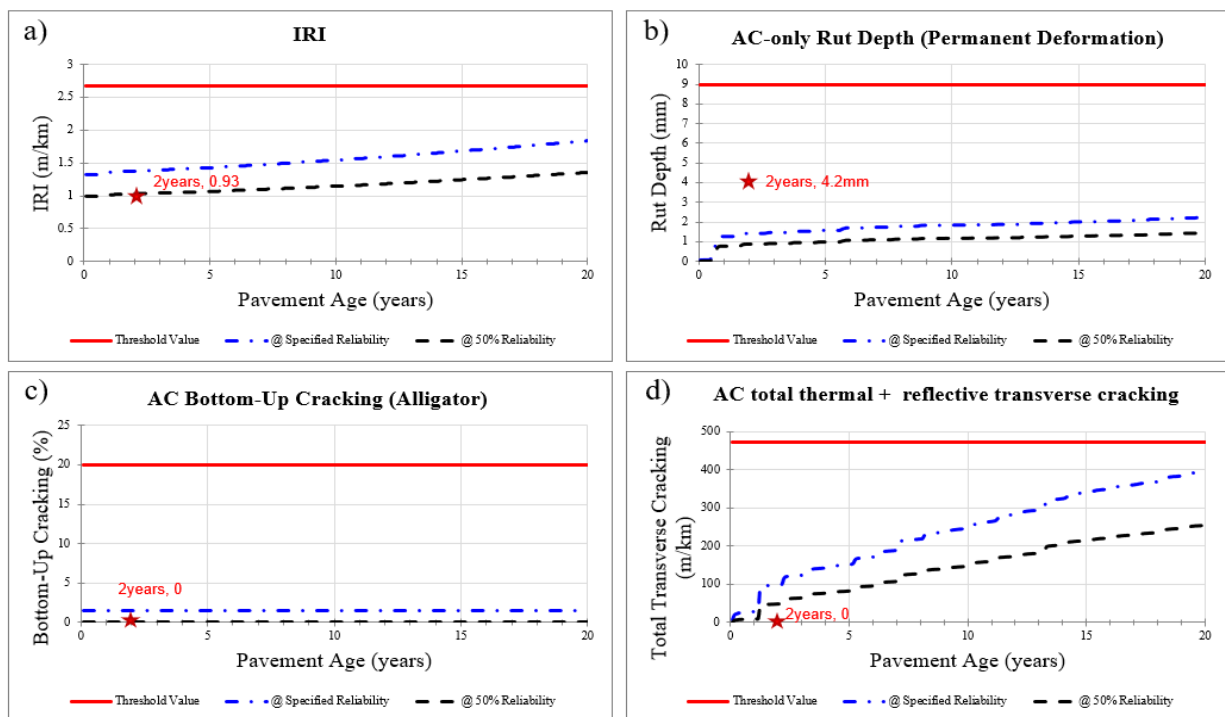


Note: Red star (*) is used to show PMS data

Figure 5.7 Mechanistic-empirical pavement design and PMS data for LD project (Tekamah)

Comparing PMS data with pavement design predictions in Figure 5.6 and Figure 5.7 shows a good level of agreement between results, which implies that the predicted designed parameters

are following the same trend as the collected data, at least during the first three years of service life. It should be noted that the discrepancies observed between predicted parameters and actual field data could be attributed to the assigned mechanical properties in some layers with level 3 of input data, deteriorations that occurred in different structural layers during many years of service life without any rehabilitation of underlying layers, construction issues at the time of pavement implementation, differences between the design traffic and climate condition and the actual conditions during service life.

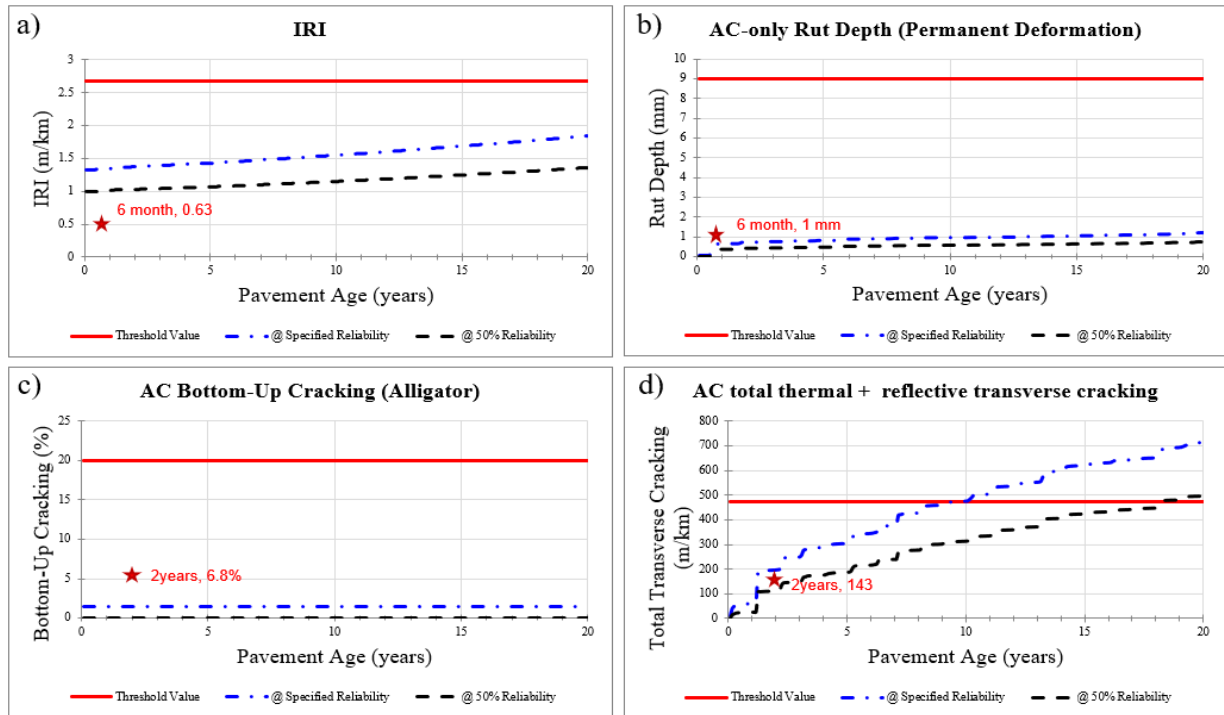


Note: Red star (*) is used to show PMS data

Figure 5.8 Mechanistic-empirical pavement design and PMS data for LE project (Grand Island)

Figure 5.8 presents the ME design for the LE project along with the PMS data collected during two years of service life. As indicated in Figure 5.3, this project also has a PCC layer underneath the pavement, which makes reflective transverse cracking the governing type of

distress on the surface, as confirmed by the design predictions. However, the MEPDG shows the overall pavement structure could potentially meet the criteria during 20 years of service life, which is supported so far by no cracking occurring during two years of service life. Additional field data still needs to be collected to further verify these design assumptions. Figure 5.9 shows the design and PMS data for the LF project, which is another pavement with PCC as one of the underlying layer structures. It is evident that reflective transverse cracking is the governing distress predicted by MEPDG, and the PMS data from the first two years of service life further verifies this design. Overall, Figure 5.6 to Figure 5.9 help verify the design assumptions used for the ME approach. With this verification, it becomes possible to take a further step and use these design parameters for each AC mixture project and underlying layers to predict the service life of each project on a reference structural layer. This approach will assist in determining the initial threshold criteria for each performance test, as detailed in the next section.



Note: Red star (*) is used to show PMS data

Figure 5.9 Mechanistic-empirical pavement design and PMS data for LF project (Ong Spur)

5.4 Defining Performance Tests' Threshold using MEPDG Approach

After verifying the design input and assumptions for the MEPDG method, the next step was to determine threshold criteria for each performance test using this approach. The initial verification considers actual site conditions (traffic, design layers, and environmental conditions) from each project location. However, to establish a threshold with a focus on asphalt mixture performance, all other variables (traffic volume, layer design, sublayer's material properties, environmental conditions) must be maintained constant in order to differentiate pavement performance based on asphalt mixture input properties. To this goal, three representative pavement structures typical of Nebraska roadways were analyzed using ME method:

1. The first representative structure (PCC structure-1st scenario) consists of a four-inch asphalt concrete (AC) surface layer over an eight-inch PCC layer, both positioned on a semi-infinite A-6 type subgrade (Figure 5.10a).
2. The second representative structure (PCC structure-2nd scenario) maintains the same PCC and subgrade configuration as the first scenario but replaces the surface layer with three inches of conventional AC mixture over one inch of fine-graded asphalt mixture (Figure 5.10b).
3. The third configuration (non-PCC structure) represents a flexible pavement consisting of three inches of AC mixture over three inches of chemically stabilized hydrated lime, followed by two inches of non-stabilized A-2-4 base material on a semi-infinite A-7-6 type subgrade (Figure 5.10c).

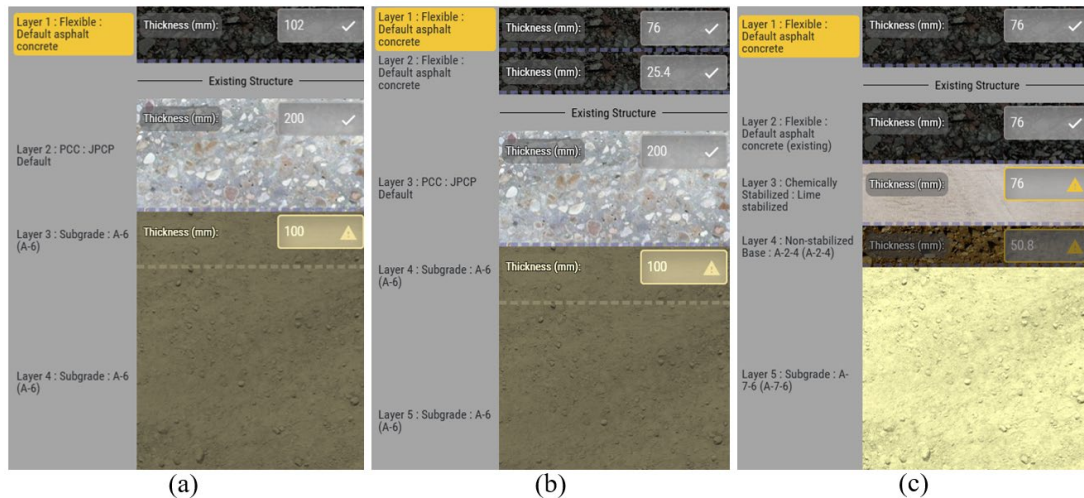


Figure 5.10 Representative structures for NE pavements: a) PCC structure-1st scenario, b) PCC structure-2nd scenario, and c) non-PCC structure

After verifying the design input and assumptions for the MEPDG method, the next step was to determine threshold criteria for each performance test using this approach. To accomplish

this, different pavements were designed by a mechanistic-empirical method using representative structures, while the top-lift layer varied based on properties of different projects (LA, LD, LE, and LF). This approach was adopted to maintain the pavement structural layer properties and capacities, traffic, and climate inputs and only change the top-lift layer properties. This way, all variables were controlled and the changes in output parameters (rut depth, cracking, etc.) were attributed solely to the AC mixture properties and associated performances.

5.4.1 PCC-Structure-1st Scenario

In the case of PCC structure-1st scenario, the ME results in terms of rutting depth and reflective transverse cracking are represented in Figure 5.11. As can be seen in Figure 5.11a, after 20 years of service life, the rutting depths do not exceed the criteria in any of the pavement projects, indicating no issues regarding rutting performance in these projects. Accordingly, the most rutting susceptible project (LA) shows only 3 mm of rut depth after 20 years of service life, which is significantly less than the threshold value of 9 mm. It should also be noted that Nebraska has never experienced major issues regarding pavement performances related to rutting distress, which further verifies the results obtained from this ME method. As such, the RT_{Index} associated with the lowest rutting resistant project (LE), with the value of 44, is selected as the preliminary criteria for RT_{Index} in pavements with PCC structures-1st scenario. However, it should be noted that this value of RT_{Index} is very conservative and it could potentially be reduced if there is a need to compensate for other types of distresses such as cracking.

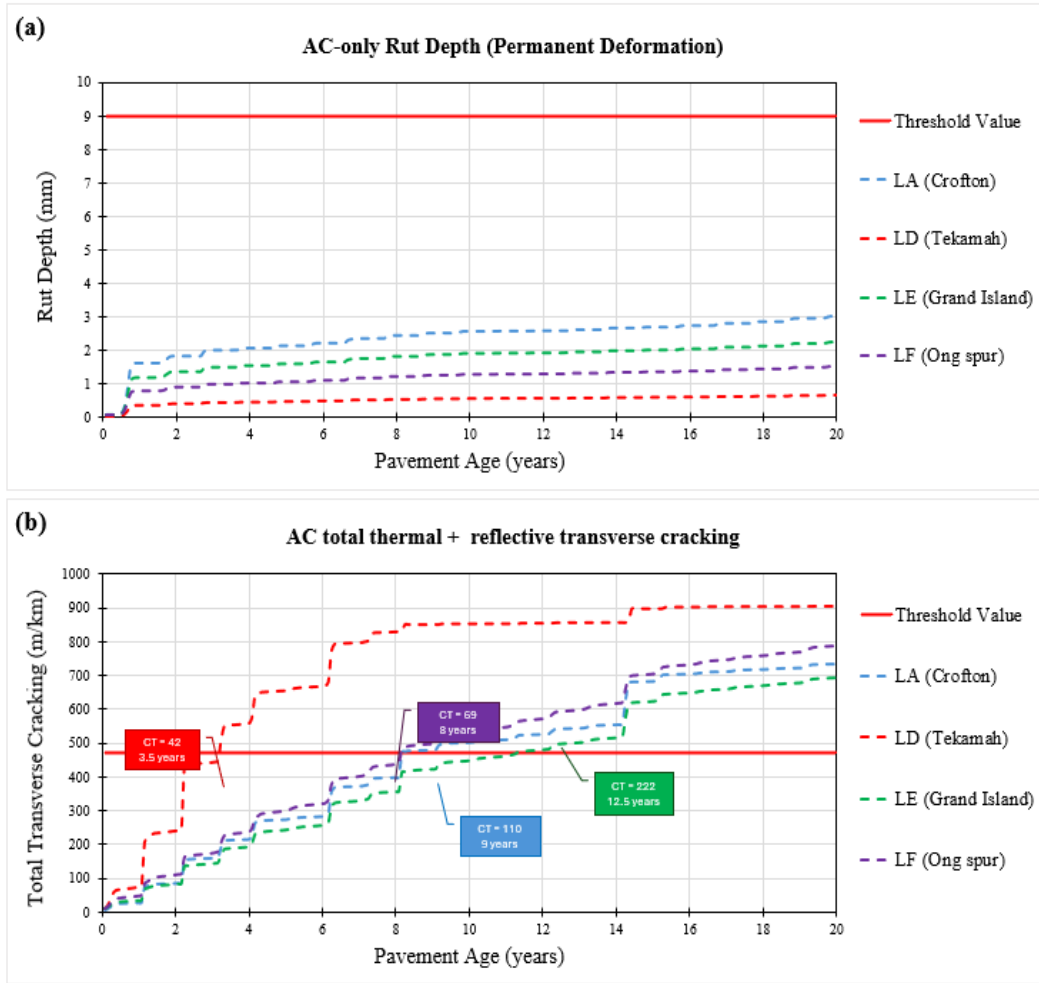


Figure 5.11 PCC structure-1st scenario: ME predicted service life for different AC mixtures a) predicted rut depth and b) predicted total reflective transverse cracking

Taking cracking damage into account, Figure 5.11b indicates that all projects exceed the threshold value at different points during the 20 years of predicted service life. The CT_{Index} associated with each project is indicated next to the graph of predicted service life, showing how long each project with a specific CT_{Index} could resist cracking damage before failure. As can be seen, LD with CT_{Index} of 42 could last 2.5 years of service life, while LE with CT_{Index} of 222 could extend up to 12.5 years of service life. Figure 5.12 shows the correlation between the CT_{Index} value and pavement service life for the PCC structure - 1st scenario. Based on the limited data in

this study, for a PCC structural layer in Nebraska and considering the 1st scenario, a minimum CT_{Index} of 100 is required to achieve eight years of service life.

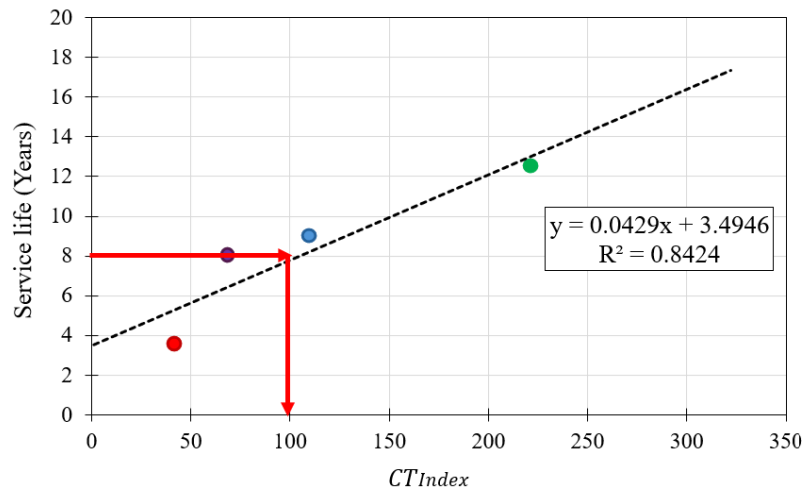


Figure 5.12 PCC structure-1st scenario: Criteria selection for IDEAL CT test based on ME approach

5.4.2 PCC-Structure-2nd Scenario (with a thin fine-graded mixture layer)

As was mentioned earlier, in the 2nd scenario, the four inches of AC layer is replaced with 3 inches of AC layer on top of one inch of fine graded asphalt mixture. As can be seen in Figure 5.13a, similar to the 1st scenario, the rutting depths do not exceed the threshold criteria in any of the pavement projects during 20 years of service life. This verifies previous outcomes that there are no issues regarding rutting performance in these projects in Nebraska. Accordingly, the RT_{Index} associated with the lowest rutting resistant project (LE), with the value of 44, is selected as the preliminary criteria for RT_{Index} in pavements with PCC structures-2nd scenario. However, similar to 1st scenario, this value of RT_{Index} is selected in a conservative way and there is room for reduction in case it could possibly reduce other types of distresses.

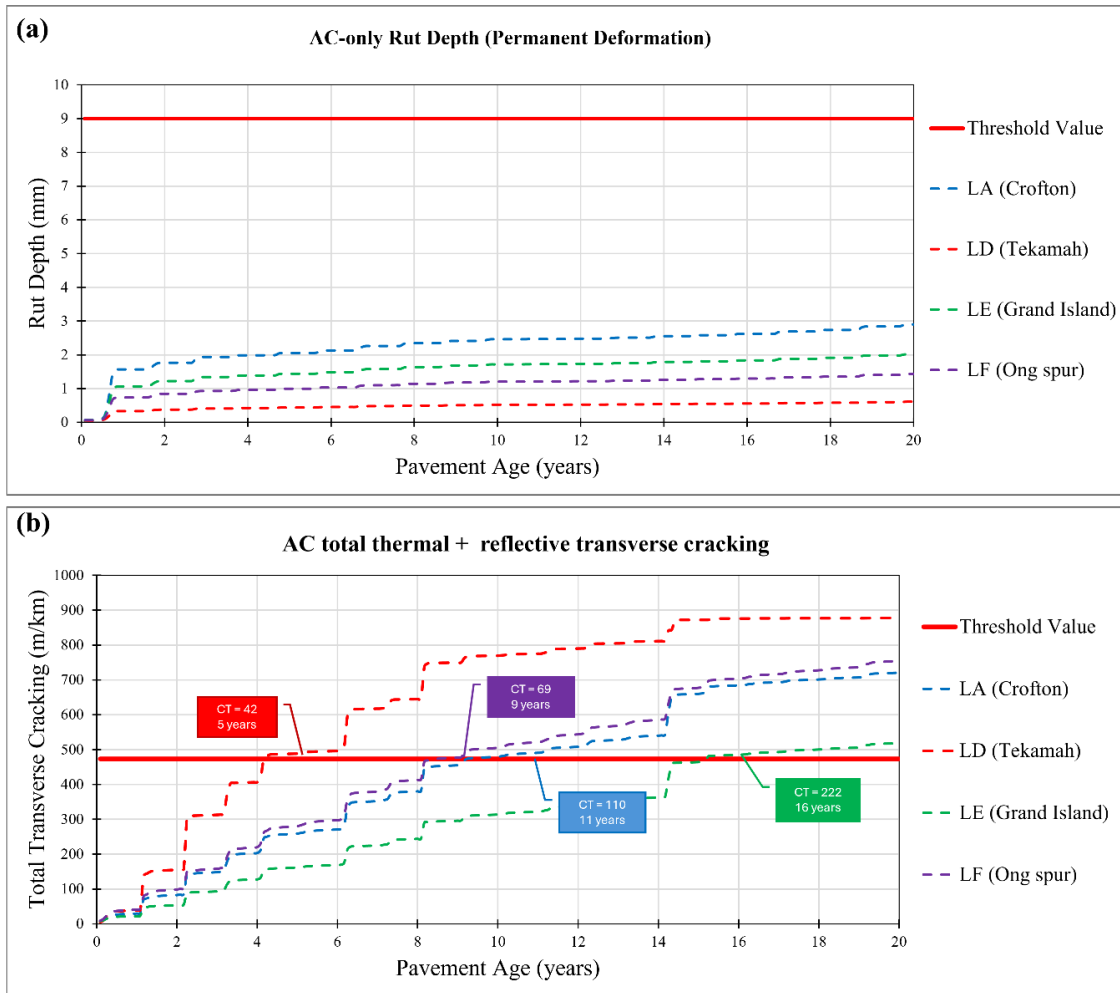


Figure 5.13 PCC structure-1st scenario: ME predicted service life for different AC mixtures a) predicted rut depth and b) predicted total reflective transverse cracking

Taking reflective transverse cracking into account, Figure 5.13b indicates that all projects exceed the threshold value at different points during the 20 years of predicted service life. The CT_{Index} associated with each project is indicated next to the graph of predicted service life, showing how long each project with a specific CT_{Index} could resist reflective cracking damage before failure. As can be seen, LD with CT_{Index} of 42 could last 5 years of service life, while LE with CT_{Index} of 222 could extend up to 16 years of service life. As it is evident, in terms of comparison between 1st and 2nd scenario of PCC structure, the 2nd scenario is showing improved

service life for all the assigned projects. Several reasons could be mentioned to support this improvement. Having a fine aggregate interlayer could affect the reflective cracking prediction models in the ME design through changes in stress distribution, modification of cracking transfer functions, and adjusting the crack propagation rate models. That said, with the new fine graded interlayer, the dynamic modulus, gradation parameters, binder content and grade, and air void content are changing compared to the 1st scenario. The modified interlayer fracture properties could affect the parameters of modified Paris' law (equation 5.6 and 5.7) accounting for crack growth. Furthermore, with the use of fine aggregate interlayer, stress concentrations at PCC joints will change by calibrating a different effective stress intensity factor. More than that, the finite element analysis used as a multi-layer elastic theory in the ME structural analysis would have different properties for the interface elements due to the presence of fine aggregate interlayer.

Figure 5.14 shows the correlation between CT_{Index} value and pavement service life for projects built on PCC structure-2nd scenario. Based on the limited data in this study, for the PCC structure-2nd scenario in Nebraska, a minimum CT_{Index} of 70 is required to achieve eight years of service life. Taking a look at literature, different states have come up with a wide range of CT_{Index} values for the criterion. Missouri defined the range of 32 to 60 for the acceptable CT_{Index} value for Superpave designed mixtures, while contractors that produce mixtures with higher CT_{Index} values (more than 60) will get bonus up to 3% in terms of contract price. Oklahoma has defined a minimum CT_{Index} of 80 as its criterion for the short-term aged mixtures regardless of virgin binder grade. Tennessee DOT defined three levels for CT_{Index} criteria: minimum of 50 for ADT of <10,000 and minimum CT_{Index} of 75 for ADT of >10,000. Also, a minimum CT_{Index} of 100 is determined for interstates and controlled access state routes. Virginia defined the minimum CT_{Index} of 70 as the criterion for short-term aged samples. Alabama has three different CT_{Index}

criteria based on the design traffic in the state. For ESALs less than 1 million a minimum CT_{Index} of 55, for ESALs between 1 to 10 million a minimum CT_{Index} of 83, and for ESALs more than 10 million a minimum CT_{Index} of 110 is determined for mix design approval. Texas DOT specified minimum CT_{Index} of 90 for short-term aged Superpave dense-graded mixtures, while a minimum of 135 was defined for SMA mixtures.

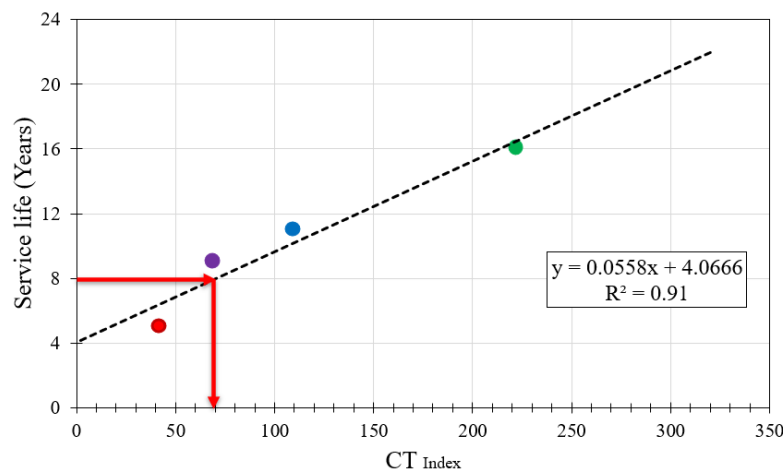


Figure 5.14 PCC structure-2nd scenario: Criteria selection for IDEAL CT based on ME approach

5.4.3 Non-PCC Structure

In the case of non-PCC structures, the pavement structural layers shown in Figure 5.10c were selected for design purposes. Figure 5.15 indicates the predicted service life for each top-lift layer constructed on top of a representative non-PCC structure. This Figure displays two main parameters associated with pavement quality for different AC projects.

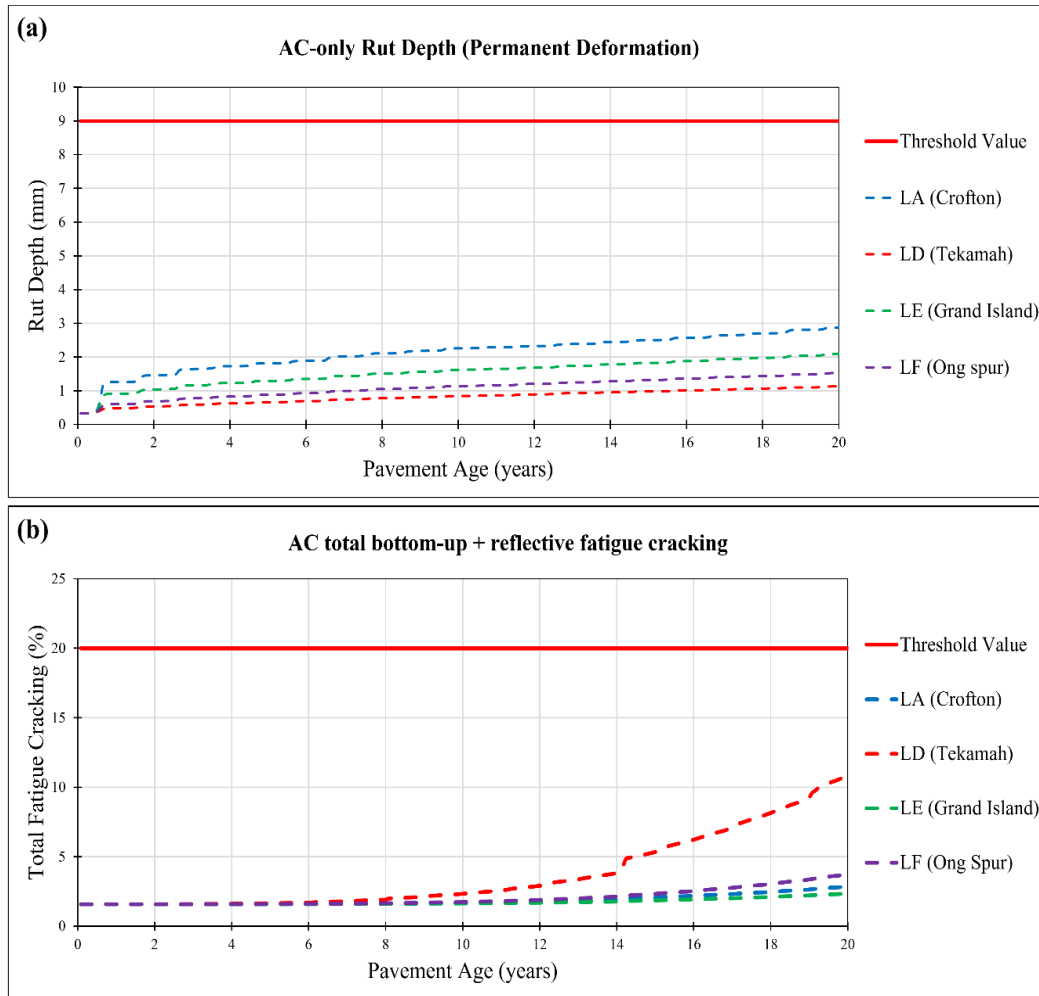


Figure 5.15 Non-PCC structure: ME predicted service life for different AC mixtures a) predicted rut depth and b) predicted total fatigue cracking

As shown in Figure 5.15, none of the designed pavements exceeded the threshold criteria associated with design parameters, which indicates that pavements implemented on top of the assumed non-PCC structures could potentially withstand 20 years of service life without major distress occurring. An important point to note is that in the non-PCC structures, reflective transverse cracking is no longer the dominant distress; instead, fatigue cracking becomes the most critical distress affecting these pavements. In the case of the LD project, based on previous

observations and laboratory tests, inferior cracking resistance was expected, which can be clearly observed in Figure 5.15b when compared to other types of AC mixtures.

Taking into account Figure 5.15, it can be concluded that for the current mix designs used in Nebraska, if non-PCC structural layers with the representative properties and capacities shown in this study are used, all the CT_{Index} and RT_{Index} values obtained in this study are overdesigning the pavement. Accordingly, some adjustments are required to improve the mix design procedure to prevent waste of materials and overdesigning of pavements with such structural layer properties. That said, no preliminary thresholds are assigned for representative non-PCC structural layers in Nebraska at this stage of the study.

Chapter 6 Long-Term Aging Protocol Selection

The last step in this study was to determine a suitable LTA protocol for potential application in the Nebraska BMD framework since the previous performance tests and threshold criteria are defined for specimens produced under STA conditions. However, long-term aging might have significant effects on mixtures' performance that could adversely affect the service life of pavements. As such, it seems reasonable to include long-term aging in the BMD framework of the state, especially since cracking is the major distress in Nebraska pavements and long-term aging is the critical condition for cracking damages.

In this phase of the Nebraska BMD study, only the development of an appropriate and practical LTA protocol was under investigation. The performance tests' criteria for the LTA conditions will be investigated and determined in future phases of the study. The goal at this stage was to develop an LTA protocol that could represent the real aging of NE mixtures while being feasible within a short and practical timeframe, particularly during quality control and quality assurance phases. As previously shown in Chapter 3, the two primary cracking tests were conducted on LTA specimens aged through NCHRP and NCAT protocols. The cracking results in Figure 4.5 and Figure 4.6 indicate that the NCAT protocol, which involves aging loose mixtures for eight hours at 135 °C, was more severe in terms of aging compared to the NCHRP protocol with five days of loose mixture aging at 135 °C.

6.1 Mechanical Test Assessment of LTA Protocol

To verify which protocol reflects the real aging that occurs during service life, long-term field data are required. These data are being collected; however, it is not possible at this time to employ field data for verification purposes in terms of a long-term aging protocol. As such, the NCHRP 09-54 protocol was considered a well-established aging protocol due to the extensive

research supporting this work. Therefore, it was decided to assess an adjusted version of the NCAT protocol with reduced aging time to determine whether this adjusted protocol could replicate the NCHRP results in terms of cracking resistance. For this purpose, an adjusted protocol, named NCAT-4h, was selected, and loose mixtures were long-term aged using this protocol. Subsequently, the IDEAL-CT was conducted on the LTA specimens with the results shown in Figure 6.1.

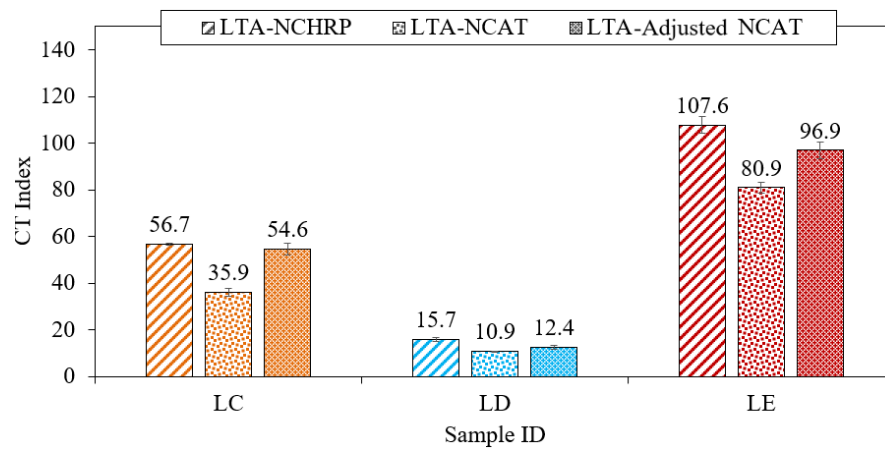


Figure 6.1 CT_{Index} for LTA specimens aged using NCHRP, NCAT, and adjusted NCAT

As can be seen in Figure 6.1, with NCAT-4h protocol, the mechanical test results obtained from IDEAL-CT are much closer to the well-established NCHRP protocol. For instance, in the case of LC, the NCHRP and NCAT-4h protocols are showing CT_{Index} values of 56.7 and 54.6, respectively. However, the results from the NCAT-8h protocol indicate 35.9 for the CT_{Index} value, which is significantly lower than the NCHRP results. These findings verified that long-term aging using the adjusted NCAT protocol could replicate the cracking results obtained from the NCHRP protocol. As such, considering mechanical performance, this LTA method can be a suitable candidate for the BMD framework.

6.2 Rheological and Chemical Test Assessment of LTA Protocol

As the asphalt mixture ages, primary changes occur in the asphalt binder properties, specifically in the chemical and rheological properties of the binder. Therefore, it is necessary to evaluate the binder properties before finalizing the LTA protocol at this stage. For this goal, the loose asphalt mixtures from three BMD projects were subjected to LTA conditioning using NCHRP, NCAT, and NCAT-4h protocols. Afterward, the asphalt binder was extracted and recovered from these aged asphalt mixtures for further investigation using chemical and rheological tests. Dynamic shear rheometer (DSR) and Fourier transform infrared spectroscopy (FTIR) tests were conducted on the extracted and recovered binders, with Glover-Rowe (G-R) and Carbonyl index (IC=O) parameters obtained from them. G-R is a parameter that assesses the mid-temperature cracking resistance of asphalt binders, in which it measures the complex shear modulus (G^*) and phase angle (δ) of asphalt binders using 8 mm-diameter geometry with a 2 mm testing gap at 45 °C and 10 rad/sec in a DSR machine [69]. The G-R parameter is determined using Equation 6.1:

$$G - R = \frac{G^* \times (\cos\delta^2)}{\sin\delta} \quad (6.1)$$

Based on the concept of the black space diagram, a binder with G-R value of less than 180 kPa will not experience any mid-temperature cracking. However, G-R values higher than 600 kPa represent binders that will experience severe cracking during service life. The damage zone is defined as the zone between the curve for 180 kPa and curve for 600 kPa [69].

The IC=O parameter is used to characterize the chemical properties of the aged binders in this study. This parameter is obtained using the FTIR technique with a key wavenumber typically around 1700 cm^{-1} . The absorption spectrum is analyzed and the areas under the peaks are estimated. The FTIR test was conducted using a Nicolet Avatar 380 FTIR spectrometer based on

the attenuated total reflection (ATR) mode. A resolution of 4 cm^{-1} within a wavenumber range of 400 to 4000 cm^{-1} was applied to record the spectra, while the OMNIC 8.1 software was further utilized to estimate the areas under the peaks. IC=O was measured following Equation 6.2:

$$IC = O = \frac{\text{Area under } 1700\text{ cm}^{-1}\text{peak}}{\text{Area under } 1400 - 1480\text{ cm}^{-1}\text{peak}} \quad (6.2)$$

The mid-temperature cracking characterization using the G-R parameter is plotted in a black space diagram and depicted in Figure 6.2. This characterization was performed on unaged binders, NCAT-4h, NCAT-8h, and NCHRP-5days aged binders. The results show that with progressive aging (increasing severity of aging), the unaged binders gradually approach the crack-initiation curve; however, none of the binders in either of these aging conditions exceeded the crack-initiation criteria. Considering the level of aging occurring in each of the LTA protocols, it is evident that the NCAT-8h protocol produces the most severe aged binders, followed by the NCHRP and NCAT-4h protocols. It is also important to note that the same pattern was observed in the mechanical test results based on the IDEAL-CT performance test.

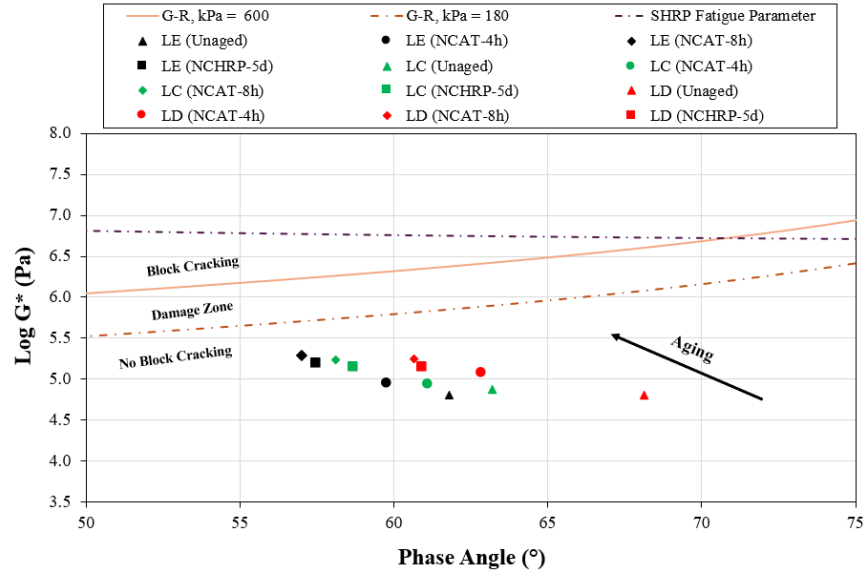


Figure 6.2 Black-space diagram: G-R test results for different binders

To further evaluate the aging severity of each LTA protocol, the G-R parameter for all the extracted binders aged under various LTA protocols is shown in Figure 6.3. As expected, the lowest G-R value in all cases belongs to unaged binders. As the binders undergo LTA conditioning, the G-R value increases, with the highest value in all three binder case studies reported for the NCAT-8h protocol. Referring to the original plan, when the NCAT-8h protocol showed greater severity compared to the well-established NCHRP method, the NCAT-4h protocol was examined to determine if it could produce the same level of aging as the NCHRP method. As can be seen in Figure 6.3, the NCAT-4h protocol is less severe in terms of aging compared to the NCHRP protocol, based on the data derived from three case studies in this research. Accordingly, it appears that an aging time between four to eight hours might be appropriate to simulate the same level of aging as the NCHRP method.

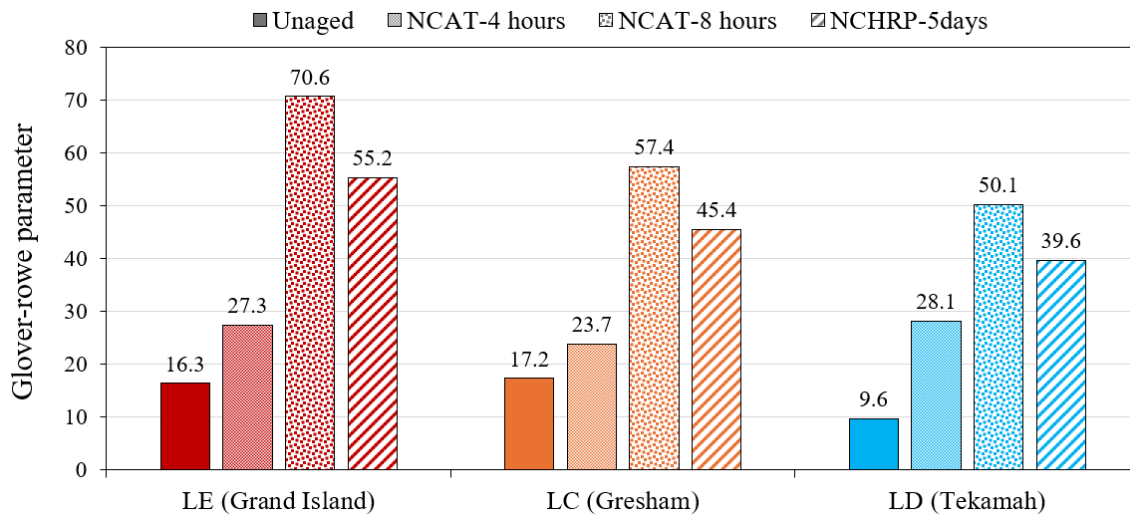


Figure 6.3 The G-R parameter for extracted binders obtained from different LTA protocols

The results for chemical characterization of binder aged within different LTA protocols, considering the IC=O parameter, are presented in Figure 6.4. As shown, the overall trend is similar to what was observed in the G-R results, which indicates that chemical and rheological properties of LTA binders follow similar patterns. Accordingly, NCAT-4h does not sufficiently age binders to simulate the NCHRP protocol, while NCAT-8h over-ages the binders. Therefore, similar to the conclusion drawn from G-R results, an aging time between four to eight hours following the same condition as the NCAT protocol might be appropriate to mimic the NCHRP aging protocol, which serves as the reference aging protocol in this study.

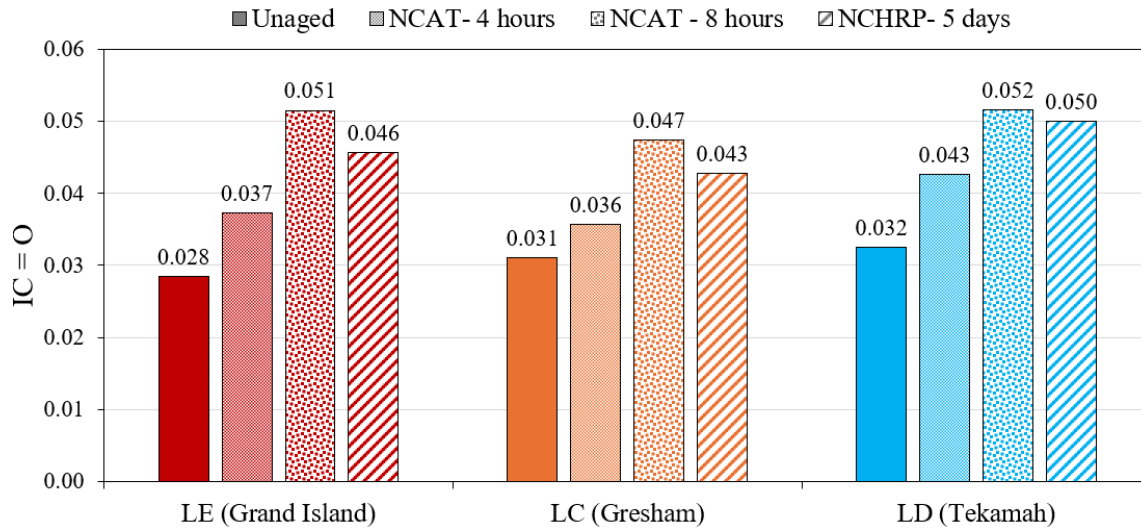


Figure 6.4 The G-R parameter for extracted binders obtained from different LTA protocols

The results from chemical and rheological analyses were used to determine the appropriate timing for the NCAT protocol that can accurately simulate the same level of aging (in both chemical and rheological terms) as the NCHRP protocol, which serves as the reference protocol in this study. To this goal, Figure 6.5 presents the NCAT conditioning graphs for time vs. G-R and time vs. IC=O parameters, based on the results from this study. As can be seen, there is a strong direct relationship between conditioning time and aging occurring in asphalt binders. The reference values for the G-R and IC=O parameters can be obtained from NCHRP aged results in Figure 6.4 and Figure 6.5, respectively. In terms of G-R, values of 55.2, 45.4, and 39.6 are recorded for LE, LC, and LD, respectively. Furthermore, IC=O values of 0.046, 0.043, and 0.050 are recorded for LE, LC, and LD, respectively. The average value for each parameter is calculated and applied in the equations shown in Figure 6.5 to determine the suitable conditioning time in the NCAT aging protocol that can simulate the equivalent level of aging that happens in the NCHRP method. Based on this analysis, 6.4 hours in NCAT conditioning is the time obtained to replicate the reference G-R parameter, while 6.8 hours is the time obtained to replicate the reference IC=O parameter.

Consequently, 6.5 hours at 135 °C was selected for the adjusted NCAT protocol that could be used in the BMD framework for Nebraska state. Further validation of this proposed protocol considering a wide range of Nebraska binders and additives is recommended.

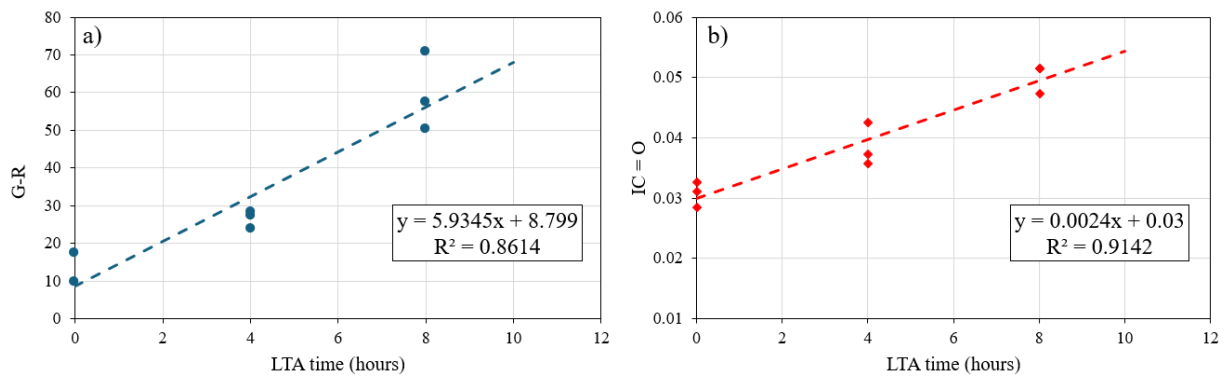


Figure 6.5 Various conditioning times for NCAT protocol: a) time vs. G-R parameter and b) time vs. IC=O parameters

Chapter 7 Research Conclusion and Future Works

Based on the findings from this study, the following terms can be concluded:

- IDEAL-RT and HWTT both effectively evaluate rutting resistance, showing a strong correlation with the DM test. IDEAL-RT could be considered for this BMD framework due to its time efficiency and potential cost-effectiveness.
- IDEAL-CT and I-FIT demonstrate a strong correlation in cracking resistance evaluation, particularly after long-term aging. Both tests seem to show acceptable variability, good discrimination potential between mixtures, and generally consistent ranking of mixture performance.
- Based on the desired characteristics, specimen preparation procedure, test speed, ease of use, and cost of equipment, the IDEAL-CT and IDEAL-RT, which share similar equipment and procedures, may offer certain advantages over the other tests evaluated in this study.
- Initial performance thresholds considering mechanistic-empirical approach are established in this study. For a representative PCC structure with four inches of AC mixture, a CT_{Index} of 100 and RT_{Index} of 44 were selected for laboratory produced short-term aged mixtures. For a representative PCC structure with three inches of AC mixture over one inch of fine graded asphalt mixture, a CT_{Index} of 70 and RT_{Index} of 44 were selected for laboratory produced short-term aged mixtures. However, these values require further validation through extended field performance data. It should be noted that the selected RT_{Index} threshold value is very conservative, and there is room for reducing this preliminary threshold if it can compensate for other mixtures' properties.
- All the studied mixtures demonstrated appropriate resistance to cracking and rutting when used within the representative non-PCC structure. The minimum values of RT_{Index} and CT_{Index} in

this study (44 and 42, respectively) are selected as the preliminary threshold values for non-PCC structural layers.

- The adjusted NCAT aging protocol with 6.5 hours of aging appears to offer practical advantages over NCHRP protocol while providing similar mechanical, rheological, and chemical properties to this well-established protocol at both mixture and binder scales. At this preliminary stage, this LTA protocol could be selected for the Nebraska BMD framework. Further research with long-term field data is required to validate and adjust this selected protocol.
- Reheating loose asphalt mixtures could be a potential factor impacting performance test criteria. It is recommended to evaluate this factor for future studies.

With that, some important steps toward advancing asphalt mixture performance tests, threshold criteria, and long-term aging conditioning protocols have been fulfilled. For future work, round-robin testing could help establish precision and bias information. Furthermore, robust validation of the tests should be conducted through benchmarking efforts and field data collection, leading to adjustments in setting up the criteria for specifications. This long-term field data could be used to adjust and modify the appropriate and practical laboratory LTA protocols.

References

- [1] E. ; Coleri and I. A. ; Sreedhar, Shashwath ; Obaid, “Development of a Balanced Mix Design Method in Oregon,” 2020.
- [2] F. Hveem, E. Zube, and J. Skog, “Proposed new tests and specifications for paving grade asphalts,” Proceeding of association of asphalt paving technologists. Accessed: May 28, 2022. [Online]. Available: <https://trid.trb.org/view/727181>
- [3] G. Huber, “History of Asphalt Mix Design in North America, Part 1: From Hubbard to Marshall,” *Asphalt*, vol. 28, no. 1, 2013.
- [4] F. Yazdipناه, M. Khedmati, and H. Haghshenas, “Nebraska Balanced Mix Design–Phase I,” 2023, Accessed: Jan. 21, 2024. [Online]. Available: <https://rosap.nhl.bts.gov/view/dot/67907>
- [5] R. J. Cominsky, R. B. (Rita B.) Leahy, and E. T. Harrigan, “Level one mix design : materials selection, compaction, and conditioning,” p. 121, 1994.
- [6] G. Nsengiyumva, Y.-R. Kim, and J. Hu, “Feasibility and Implementation of Balanced Mix Design in Nebraska,” *Nebraska Department of Transportation Research Reports*, 2020, Accessed: May 27, 2022. [Online]. Available: <https://digitalcommons.unl.edu/ndor/258>
- [7] R. West, F. Yin, C. Rodezno, and A. Taylor, “Balanced Mixture Design Implementation Support,” 2021.
- [8] P. By *et al.*, “Testing protocols to ensure performance of high asphalt binder replacement mixes using RAP and RAS,” 2015, Accessed: May 27, 2022. [Online]. Available: <http://www.ideals.illinois.edu/handle/2142/88680>
- [9] H. Haghshenas, H. Nabizadeh, Y.-R. Kim, and K. Santosh, “Research on high-rap asphalt mixtures with rejuvenators and WMA additives,” p. 146, 2016, Accessed: May 27, 2022. [Online]. Available: <https://digitalcommons.unl.edu/cgi/viewcontent.cgi?article=1158&context=ndor>
- [10] J. Sias Daniel and A. J. Lachance S Daniel, “Mechanistic and Volumetric Properties of Asphalt Mixtures with Recycled Asphalt Pavement,” *Transportation Research Record: Journal of the Transportation Research Board*, vol. 1929, no. 1, pp. 28–36, Jan. 2005, doi: 10.1177/0361198105192900104.
- [11] M. Ameri, A. Afshin, M. Ebrahimzadeh Shiraz, and F. Yazdipناه, “Effect of wax-based warm mix additives on fatigue and rutting performance of crumb rubber modified asphalt,” *Constr Build Mater*, vol. 262, 2020, doi: 10.1016/j.conbuildmat.2020.120882.
- [12] M. Ameri, F. Yazdipناه, A. Rahimi Yengejeh, and A. Afshin, “Production temperatures and mechanical performance of rubberized asphalt mixtures modified with two warm mix asphalt (WMA) additives,” *Materials and Structures/Materiaux et Constructions*, vol. 53, no. 4, Aug. 2020, doi: 10.1617/s11527-020-01542-4.

- [13] A. K. Apeagyei, "Laboratory evaluation of antioxidants for asphalt binders," *Constr Build Mater*, vol. 25, no. 1, pp. 47–53, 2011, doi: 10.1016/j.conbuildmat.2010.06.058.
- [14] J. L. Goodrich, "Asphalt and Polymer Modified Asphalt Properties Related to the Performance of Asphalt Concrete Mixes," *Journal of Association of Asphalt Paving Technologists*, vol. 57, pp. 116–160, 1988, Accessed: May 27, 2022. [Online]. Available: <https://trid.trb.org/view/486635>
- [15] G. M. Nsengiyumva, K. Santosh, Y. R. Kim, H. Xu, ..., and Y. Yang, "New Mixture Additives for Sustainable Bituminous Pavements," 2018, Accessed: May 27, 2022. [Online]. Available: <https://works.bepress.com/gabriel-nsengiyumva/1/download/%0Ahttps://digitalcommons.unl.edu/ndor/225/>
- [16] E. Coleri, S. Sreedhar, S. Haddadi, and B. Wruck, "Adjusting asphalt mixes for increased durability and implementation of a performance tester to evaluate fatigue cracking of asphalt concrete," p. 224, 2018, Accessed: May 27, 2022. [Online]. Available: https://www.oregon.gov/ODOT/Programs/ResearchDocuments/SPR785_DurabilityCracking.pdf
- [17] F. Zhou, S. Hu, G. Das, and T. Scullion, "High RAP Mixes Design Methodology with Balanced Performance," *Fhwa/Tx-11/0-6092-2*, vol. 7, no. 2, pp. 1–46, 2011, Accessed: May 27, 2022. [Online]. Available: <http://tti.tamu.edu/documents/0-6092-2.pdf>
- [18] F. Zhou, S. Hu, and T. Scullion, "Integrated Asphalt (Overlay) Mixture Design, Balancing Rutting and Cracking Requirements," *Publication NO FHWA/TX-06/0-5123-1 2. FHWA, U.S. Department of Transportation*, vol. 7, no. 2, p. 162, 2006, Accessed: May 27, 2022. [Online]. Available: <https://static.tti.tamu.edu/tti.tamu.edu/documents/0-5123-1.pdf>
- [19] S. D. Diefenderfer and B. F. Bowers, "Initial Approach to Performance (Balanced) Mix Design: The Virginia Experience," *Transp Res Rec*, vol. 2673, no. 2, pp. 335–345, Feb. 2019, doi: 10.1177/0361198118823732.
- [20] J. Habbouche, I. Boz, and S. D. Diefenderfer, "Validation of Performance-Based Specifications for Surface Asphalt Mixtures in Virginia," *Transp Res Rec*, vol. 2676, no. 5, pp. 277–296, May 2022, doi: 10.1177/03611981211056639.
- [21] J. Harvey, R. Wu, J. Signore, ... I. B.-T., and undefined 2014, "Performance-based specifications: California experience to date," *trid.trb.org* JT Harvey, R Wu, J Signore, I Basheer, S Holikatti, P Vacura, TJ Holland *Transportation Research Circular, 2014*•*trid.trb.org*, Accessed: Mar. 05, 2024. [Online]. Available: <https://trid.trb.org/view/1400014>
- [22] by N. Louay Mohammad, M. Kim, and H. Challa, "Development of performance-based specifications for Louisiana asphalt mixtures," 2016, Accessed: Mar. 05, 2024. [Online]. Available: <https://rosap.nhtl.bts.gov/view/dot/61231>

- [23] S. Sreedhar, E. Coleri, I. A. Obaid, and V. Kumar, “Development of a Balanced Mix Design Method in Oregon to Improve Long-Term Pavement Performance,” <https://doi.org/10.1177/03611981211032222>, vol. 2675, no. 12, pp. 1121–1137, Aug. 2021, doi: 10.1177/03611981211032222.
- [24] R. West, C. Rodezno, F. Leiva, F. Y.-P. NCHRP, and undefined 2018, “Development of a framework for balanced mix design,” *eng.auburn.edu*, 2018, Accessed: Apr. 26, 2023. [Online]. Available: <https://www.eng.auburn.edu/research/centers/ncat/files/NCHRP-20-07-Task-406-BMD-Framework-Final-Report.pdf>
- [25] F. Yin, A. Taylor, ... N. T.-T. N. C. for, and undefined 2020, “Performance testing for quality control and acceptance OF balanced mix design,” *eng.auburn.edu*, 2020, Accessed: Mar. 16, 2023. [Online]. Available: <https://www.eng.auburn.edu/research/centers/ncat/files/technical-reports/rep20-02.pdf>
- [26] F. Zhou, S. Hu, and D. Newcomb, “Development of a performance-related framework for production quality control with ideal cracking and rutting tests,” *Constr Build Mater*, vol. 261, p. 120549, Nov. 2020, doi: 10.1016/j.conbuildmat.2020.120549.
- [27] F. Yazdipناه, M. Khedmati, R. Rea, J. Teixeira, and H. F. Haghshenas, “Development of a balance mix performance framework for assessing high-recycled asphalt mixtures’ resistance: a study integrating laboratory and field findings,” *Road Materials and Pavement Design*, 2025, doi: 10.1080/14680629.2025.2465577.
- [28] R. West, C. Rodezno, F. Leiva, and A. Taylor, “Regressing Air Voids for Balanced HMA Mix Design. Proj NCHRP 20-07/Task 406.,” no. 0092, pp. 7–20, 2018, Accessed: May 27, 2022. [Online]. Available: <https://rosap.nrl.bts.gov/view/dot/40787>
- [29] I. L. Al-Qadi, I. M. Said, U. M. Ali, and J. R. Kaddo, “Cracking prediction of asphalt concrete using fracture and strength tests,” *International Journal of Pavement Engineering*, Aug. 2022, doi: 10.1080/10298436.2021.1892108.
- [30] T. Bennert, E. Haas, ... E. W.-... : association of asphalt, and undefined 2021, “Indirect tensile testing for balanced mixture design and quality control performance testing,” *researchwithrutgers.com* T Bennert, E Haas, E Wass, B Berger *Asphalt paving technology: association of asphalt paving, 2021*•*researchwithrutgers.com*, Accessed: Mar. 05, 2024. [Online]. Available: <https://www.researchwithrutgers.com/en/publications/indirect-tensile-testing-for-balanced-mixture-design-and-quality->
- [31] I. L. Al-Qadi *et al.*, “Development of long-term aging protocol for implementation of the Illinois flexibility index test (I-FIT),” *ideals.illinois.edu* IL Al-Qadi, H Ozer, Z Zhu, P Singhvi, U Mohamed Ali, M Sawalha, AF Espinoza Luque *FHWA-ICT-19-009, 2019*•*ideals.illinois.edu*, 2019, Accessed: Mar. 05, 2024. [Online]. Available: <https://www.ideals.illinois.edu/items/111764>
- [32] “Special Specification 3074 Superpave Mixtures-Balanced Mix Design”.

- [33] W. King and M. Kabir, "Testing and analysis of LWT and SCB properties of asphaltic concrete mixtures.," 2011, Accessed: Mar. 09, 2025. [Online]. Available: <https://rosap.ntl.bts.gov/view/dot/22276>
- [34] C. Chen, F. Yin, P. Turner, R. C. West, and N. Tran, "Selecting a laboratory loose mix aging protocol for the NCAT top-down cracking experiment," *Transp Res Rec*, vol. 2672, no. 28, pp. 359–371, Jan. 2018, doi: 10.1177/0361198118790639.
- [35] Y. R. Kim, C. Castorena, N. F. Saleh, E. Braswell, M. Elwardany, and F. Y. Rad, "Long-Term Aging of Asphalt Mixtures for Performance Testing and Prediction: Phase III Results," *Long-Term Aging of Asphalt Mixtures for Performance Testing and Prediction: Phase III Results*, Nov. 2021, doi: 10.17226/26133.
- [36] "SECTION 1028 -- SUPERPAVE ASPHALTIC CONCRETE." Accessed: Oct. 20, 2024. [Online]. Available: <https://www.yumpu.com/en/document/view/36361309/section-1028-superpave-asphaltic-concrete>
- [37] R. L. Lytton, J. Uzan, E. G. Femando, R. Roque, D. Hiltunen, and S. M. Stoffels, *Development and validation of performance prediction models and specifications for asphalt binders and paving mixes*. 1993. Accessed: Mar. 09, 2025. [Online]. Available: <https://onlinepubs.trb.org/onlinepubs/shrp/SHRP-A-357.pdf>
- [38] L. Francken, C. C.-P. of: M. University, A. Arbor, and undefined 1987, "CHARACTERIZATION AND STRUCTURAL ASSESSMENT OF BOUND MATERIALS FOR FLEXIBLE ROAD STRUCTURES. SIXTH INTERNATIONAL CONFERENCE," *trid.trb.org*, Accessed: Mar. 09, 2025. [Online]. Available: <https://trid.trb.org/View/302923>
- [39] F. Zhou, S. Im, L. Sun, and T. Scullion, "Development of an IDEAL cracking test for asphalt mix design and QC/QA," *Asphalt Paving Technology: Association of Asphalt Paving Technologists-Proceedings of the Technical Sessions*, vol. 86, pp. 549–577, 2017, doi: 10.1080/14680629.2017.1389082.
- [40] Y. Kim, C. Castorena, N. Saleh, and E. Braswell, *Long-term aging of asphalt mixtures for performance testing and prediction: Phase III results*. 2021. Accessed: Mar. 14, 2023. [Online]. Available: <https://trid.trb.org/view/1846357>
- [41] "AASHTO T 378 - Standard Method of Test for Determining the Dynamic Modulus and Flow Number for Asphalt Mixtures Using the Asphalt Mixture Performance Tester (AMPT) | GlobalSpec." Accessed: May 13, 2024. [Online]. Available: <https://standards.globalspec.com/std/10182831/aashto-t-378>
- [42] "Standard Method of Test for Hamburg Wheel-Track Testing of Compacted Hot Mix Asphalt (HMA)", Accessed: Mar. 26, 2023. [Online]. Available: www.matest.ru
- [43] T. Manual, R. Documents, S. A. Mixtures, U. S. S. Specimens, A. Mixtures, and A. Mixtures, "ALDOT-458 High Temperature Indirect Tensile Test for HMA," pp. 5–8, 2020.

- [44] “AASHTO - T 393 - Standard Method of Test for Determining the Fracture Potential of Asphalt Mixtures Using the Illinois Flexibility Index Test (I-FIT).” Accessed: Oct. 12, 2023. [Online]. Available: <https://standards.globalspec.com/std/14554354/T%20393>
- [45] “D8225 Standard Test Method for Determination of Cracking Tolerance Index of Asphalt Mixture Using the Indirect Tensile Cracking Test at Intermediate Temperature.” Accessed: May 13, 2024. [Online]. Available: <https://www.astm.org/d8225-19.html>
- [46] from Y. Richard Kim *et al.*, “NCHRP 09-54 Long-Term Aging of Asphalt Mixtures for Performance Testing and Prediction,” 2015.
- [47] A. K. Apeagyei, “Correlating rutting with dynamic modulus of asphalt concrete,” *Proceedings of the Institution of Civil Engineers: Transport*, vol. 164, no. 4, pp. 241–249, 2011, doi: 10.1680/TRAN.9.00056.
- [48] P. By, I. L. Al-Qadi, Q. Aurangzeb, S. H. Carpenter, W. J. Pine, and J. Trepanier, “Impact of High RAP Contents on Structural and Performance Properties of Asphalt Mixtures,” *FHWA-ICT-12-002*, 2012, Accessed: Jun. 17, 2024. [Online]. Available: <https://hdl.handle.net/2142/45810>
- [49] J. R. Willis, R. West, and M. Marasteanu, *Improved mix design, evaluation, and materials management practices for hot mix asphalt with high reclaimed asphalt pavement content*. 2013. Accessed: Dec. 06, 2022. [Online]. Available: [https://books.google.com/books?hl=en&lr=&id=8PTBcbcZNX0C&oi=fnd&pg=PP1&dq=West,+R.+C.,+Rada,+G.+R.,+Willis,+J.+R.,+and+Marasteanu,+M.+O.+\(2013\).+%22Improved+mix+design,+evaluation,+and+materials+management+practices+for+hot+mix+asphalt+with+high+reclaimed++asphalt+pavement+content%22+National+Cooperative+Highway+Research+Program,+N&ots=FcGS3aeIDh&sig=RO3YpIKJ_XfDaGbPaj_F1TD00w0](https://books.google.com/books?hl=en&lr=&id=8PTBcbcZNX0C&oi=fnd&pg=PP1&dq=West,+R.+C.,+Rada,+G.+R.,+Willis,+J.+R.,+and+Marasteanu,+M.+O.+(2013).+%22Improved+mix+design,+evaluation,+and+materials+management+practices+for+hot+mix+asphalt+with+high+reclaimed++asphalt+pavement+content%22+National+Cooperative+Highway+Research+Program,+N&ots=FcGS3aeIDh&sig=RO3YpIKJ_XfDaGbPaj_F1TD00w0)
- [50] R. Zhang, J. E. Sias, and E. V. Dave, “Evaluation of the cracking and aging susceptibility of asphalt mixtures using viscoelastic properties and master curve parameters,” *Journal of Traffic and Transportation Engineering (English Edition)*, vol. 9, no. 1, pp. 106–119, Feb. 2022, doi: 10.1016/J.JTTE.2020.09.002.
- [51] C. Ogbo, F. Kaseer, M. Oshone, J. E. Sias, and A. E. Martin, “Mixture-based rheological evaluation tool for cracking in asphalt pavements,” *Road Materials and Pavement Design*, vol. 20, no. sup1, pp. S299–S314, Apr. 2019, doi: 10.1080/14680629.2019.1592010.
- [52] J. S. Daniel *et al.*, “Comparison of asphalt mixture specimen fabrication methods and binder tests for cracking evaluation of field mixtures,” *Taylor & Francis JS Daniel, M Corrigan, C Jacques, R Nemati, EV Dave, A Congalton Road Materials and Pavement Design, 2019•Taylor & Francis*, vol. 20, no. 5, pp. 1059–1075, Jul. 2019, doi: 10.1080/14680629.2018.1431148.
- [53] F. Yin, C. Chen, R. West, A. E. Martin, and E. Arambula-Mercado, “Determining the Relationship Among Hamburg Wheel-Tracking Test Parameters and Correlation to Field

- Performance of Asphalt Pavements,” *Transp Res Rec*, vol. 2674, no. 4, pp. 281–291, Apr. 2020, doi: 10.1177/0361198120912430.
- [54] A. Margaritis, ... J. B.-R. M. and, and undefined 2019, “Evaluating the mechanical performance of Flemish bituminous mixtures containing RA by statistical analysis,” *Taylor & Francis A Margaritis, J Blom, W Van den bergh Road Materials and Pavement Design, 2019*•Taylor & Francis, vol. 20, no. sup2, pp. S725–S739, Jul. 2019, doi: 10.1080/14680629.2019.1628431.
- [55] F. Yin and R. West, “Balanced mix design resource guide,” 2021, Accessed: Mar. 02, 2023. [Online]. Available: <https://trid.trb.org/view/1842890>
- [56] S. Sreedhar and E. Coleri, “Effects of Binder Content, Density, Gradation, and Polymer Modification on Cracking and Rutting Resistance of Asphalt Mixtures Used in Oregon,” *Journal of Materials in Civil Engineering*, vol. 30, no. 11, Nov. 2018, doi: 10.1061/(ASCE)MT.1943-5533.0002506.
- [57] S. Tarbox, H. Drive, J. S. Daniel, S. Tarbox, and J. Sias Daniel, “Effects of long-term oven aging on reclaimed asphalt pavement mixtures,” *journals.sagepub.com S Tarbox, JS Daniel Transportation research record, 2012*•journals.sagepub.com, vol. 2294, no. 2294, pp. 1–15, Dec. 2012, doi: 10.3141/2294-01.
- [58] R. Moraes, F. Yin, C. Chen, A. Andriescu, D. J. Mensching, and N. Tran, “Evaluation of long-term oven aging protocols on field cracking performance of asphalt binders containing reclaimed asphaltic materials (RAP/RAS),” <https://doi.org/10.1080/14680629.2023.2181004>, pp. 1–14, Mar. 2023, doi: 10.1080/14680629.2023.2181004.
- [59] A. Seittlari, I. Boz, J. Habbouche, and S. D. Diefenderfer, “Assessment of cracking performance indices of asphalt mixtures at intermediate temperatures,” *International Journal of Pavement Engineering*, vol. 23, no. 1, pp. 70–79, 2022, doi: 10.1080/10298436.2020.1730838.
- [60] I. Al-Qadi, I. Said, ... U. A.-I. J. of, and undefined 2022, “Cracking prediction of asphalt concrete using fracture and strength tests,” *Taylor & Francis IL Al-Qadi, IM Said, UM Ali, JR Kaddo International Journal of Pavement Engineering, 2022*•Taylor & Francis, vol. 23, no. 10, pp. 3333–3345, 2021, doi: 10.1080/10298436.2021.1892108.
- [61] J. E. S. L. Teixeira, C. M. Amaecing Junior, L. R. de Rezende, V. T. F. Castelo Branco, and Y. R. Kim, “Evaluation of asphalt concrete’s fatigue behavior using cyclic semi-circular bending test,” *Constr Build Mater*, vol. 400, Oct. 2023, doi: 10.1016/j.conbuildmat.2023.132772.
- [62] S. Sreedhar and E. Coleri, “The effect of long-term aging on fatigue cracking resistance of asphalt mixtures,” <https://doi.org/10.1080/10298436.2020.1745206>, vol. 23, no. 2, pp. 308–320, 2020, doi: 10.1080/10298436.2020.1745206.

- [63] F. Yin, E. Arámbula-Mercado, A. E. Martin, D. Newcomb, N. Tran, and A. Epps Martin, “Long-term ageing of asphalt mixtures,” *Taylor & Francis*, vol. 18, no. S1, pp. 2–27, Jan. 2017, doi: 10.1080/14680629.2016.1266739.
- [64] “Mechanistic-Empirical Pavement Design Guide ~ A Manual of Practice ~,” 2020.
- [65] R. Lytton, J. Uzan, E. Fernando, R. Roque, and D. Hiltunen, *Development and validation of performance prediction models and specifications for asphalt binders and paving mixes*. 1993. Accessed: Apr. 02, 2025. [Online]. Available: <https://onlinepubs.trb.org/onlinepubs/shrp/SHRP-A-357.pdf>
- [66] “2018 Pavement Design Section Materials and Research Division NDOT Pavement Design Manual”.
- [67] G. W.-T. R. Record and undefined 1990, “Dynamic testing of Nebraska soils and aggregates,” *trid.trb.org*, Accessed: Mar. 09, 2025. [Online]. Available: <https://trid.trb.org/View/352766>
- [68] H. L. Von Quintus and M. Symons, “Airfield Asphalt Pavement Technology Program Technical Guide AAPTP 05-04 Techniques for Mitigation of Reflective Cracks Principal Investigator ACKNOWLEDGMENT OF SPONSORSHIP,” 2009.
- [69] “Rowe, G. M. Prepared discussion for the AAPT paper... - Google Scholar.” Accessed: Mar. 09, 2025. [Online]. Available: https://scholar.google.com/scholar?hl=en&as_sdt=0%2C28&q=Rowe%2C+G.+M.+Prepared+discussion+for+the+AAPT+paper+by+Anderson+et+al.+Evaluation+of+the+Relationship+Between+Asphalt+Binder+Properties+and+Non-Load+Related+Crack+ing.+Journal+of+the+Association+of+Asphalt+Paving+Technologists%2C+Vol.+80%2C+2011%2C+pp.+649%E2%80%93662&btnG=